CR ANISOTROPY AS A PROBE OF CR TRANSPORT & INTERSTELLAR MAGNETIC FIELDS

Gwenael Giacinti (MPIK Heidelberg)

GG, In Prep. (2019) – *see also arXiv:1810.06396*

GG & Kirk, ApJ 835, 258 (2017), *arXiv:1610.06134*

GG & Sigl, Phys. Rev. Lett. 109, 071101 (2012), *arXiv:1111.2536*

MAX-PLANCK-INSTITUT
FÜR KERNPHYSIK
HEIDELBERG

CR Anisotropy

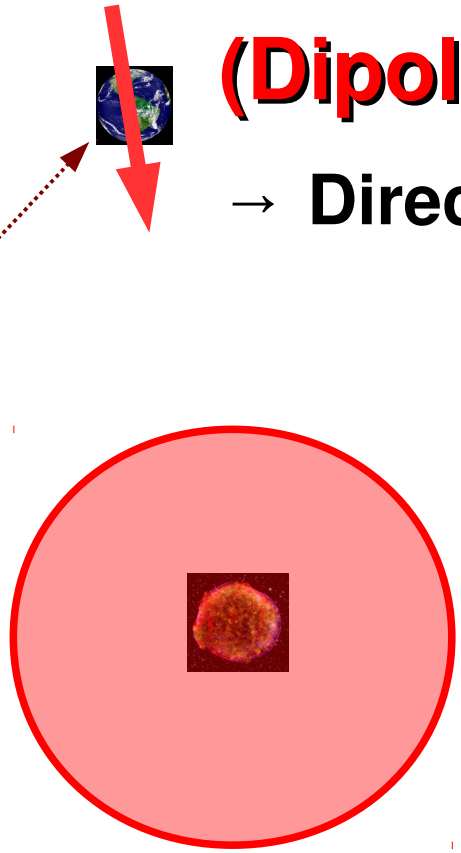

(Dipole) Anisotropy

→ **Direction**

Amplitude

$$\boldsymbol{\delta}(p) \simeq -\frac{3}{c_0}\frac{\mathbf{j}}{n} = \frac{3D(p)}{c_0}\frac{\boldsymbol{\nabla} n}{n}$$

where $\mathbf{j}(\mathbf{r}, p) = -D(p)\boldsymbol{\nabla} n$ is the CR current

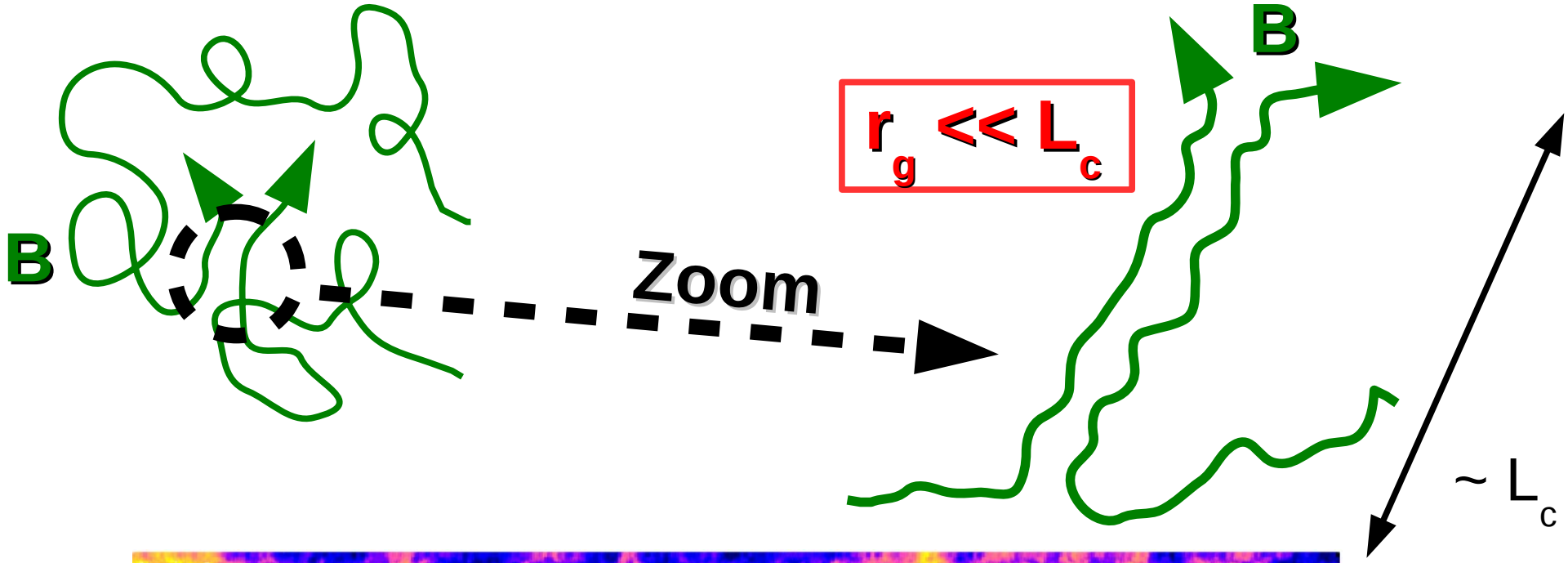
B
Zoom
$r_g << L_c$
B
~ L_c

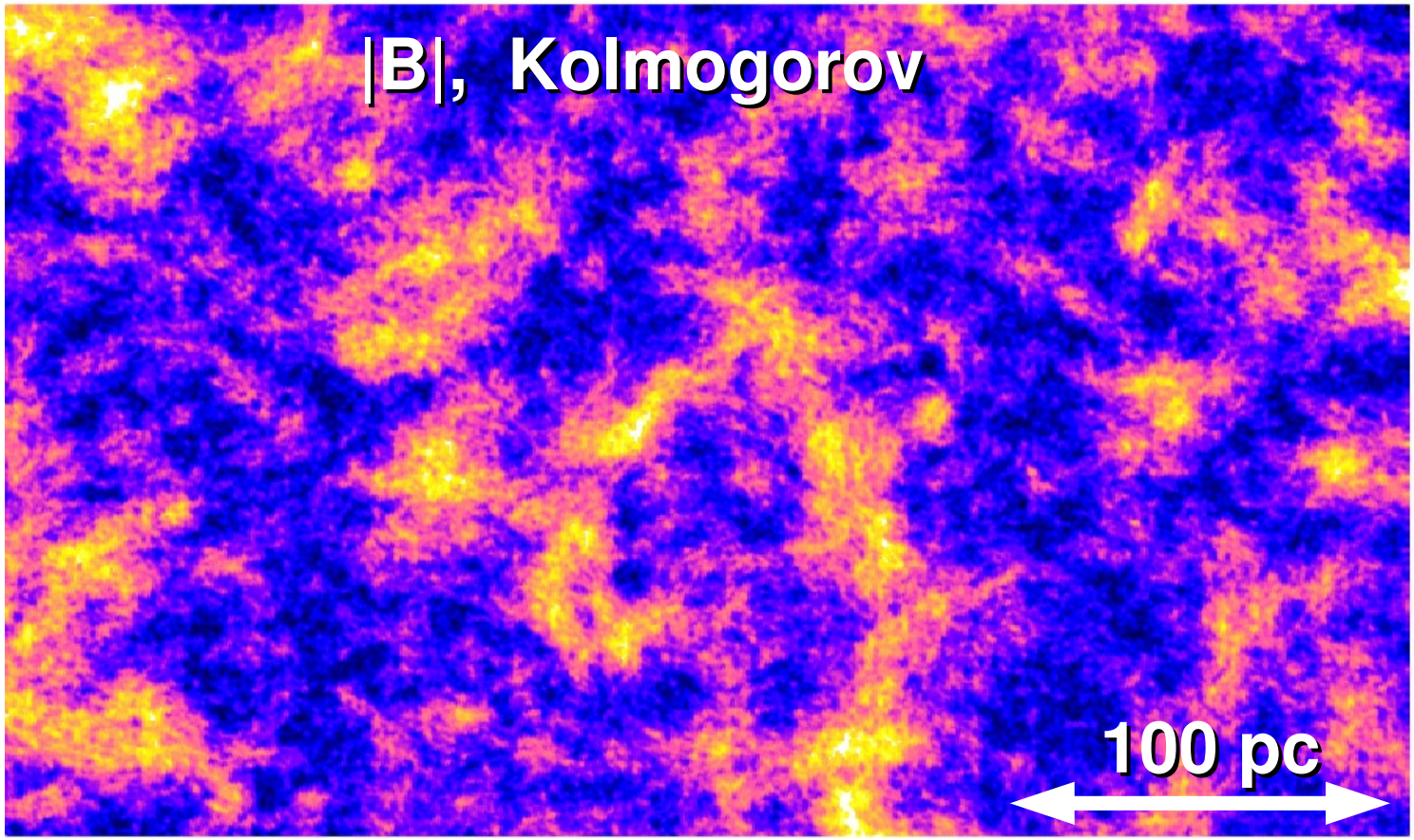
|B|, Kolmogorov
100 pc

CR Anisotropy

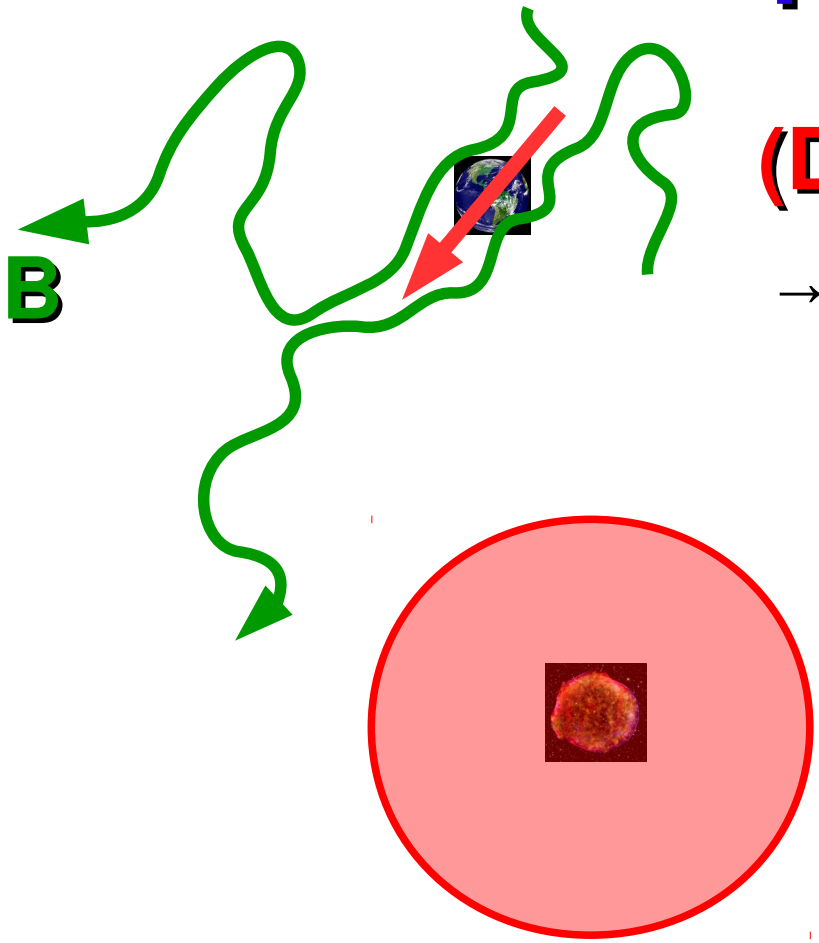

(Dipole) Anisotropy

→ **Direction B field**

cf. Schwadron et al., Science (2014)

Flip at 100 TeV : *cf. Ahlers, PRL (2016)*

Observations :

Large Scale Anisotropy (~0.1%) :

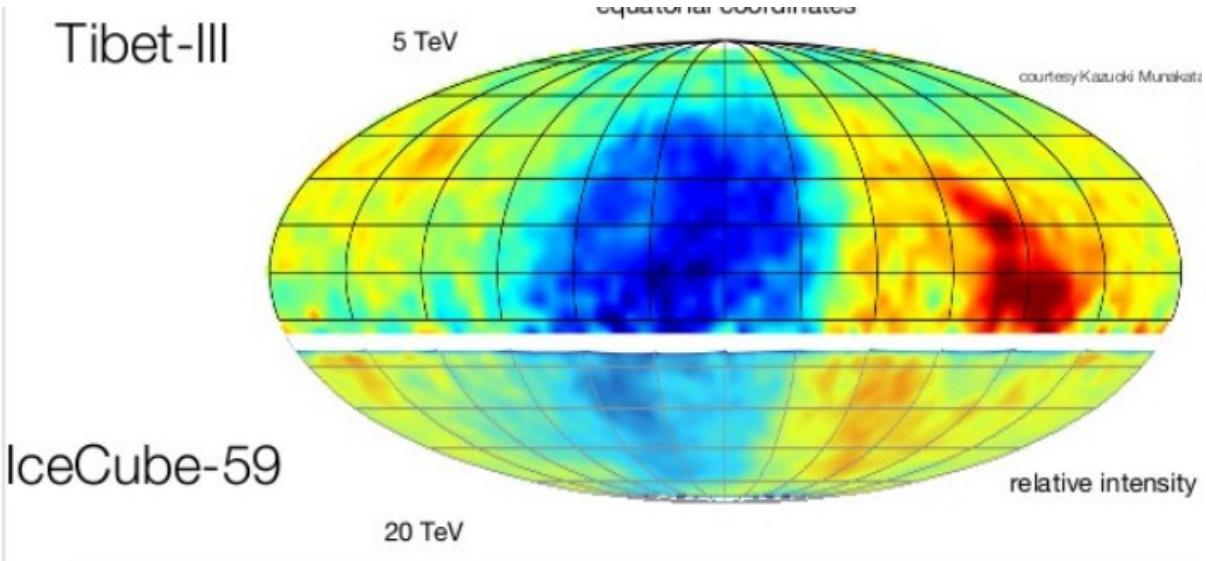

Cl [arXiv:1708.03005]:

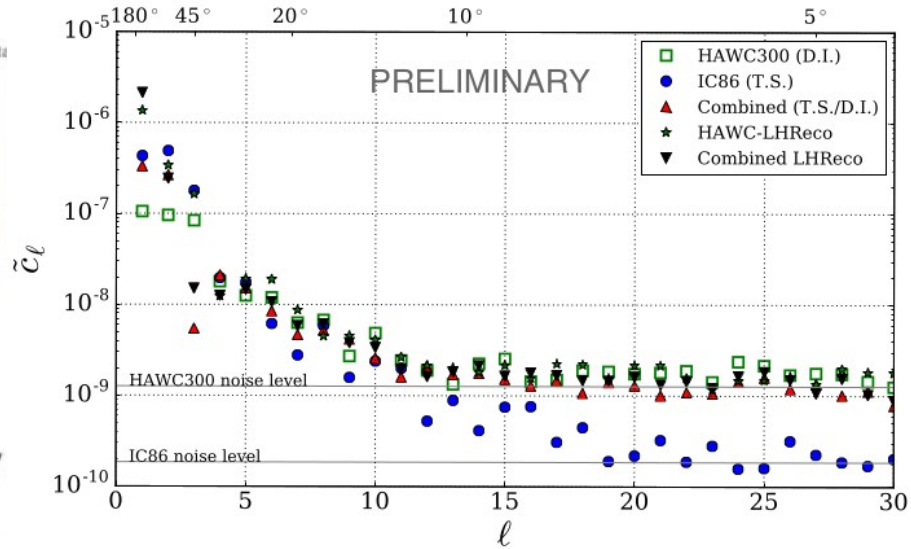

Small Scale Anisotropies (~0.01%) :

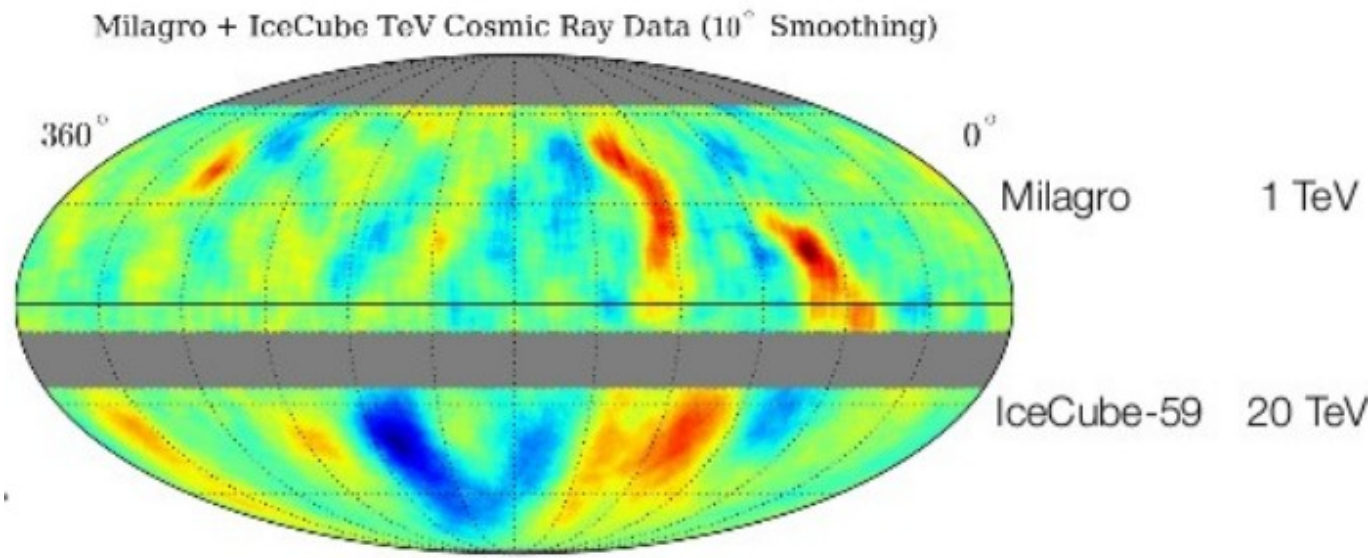

Pitch-angle (θ) and gyrophase:

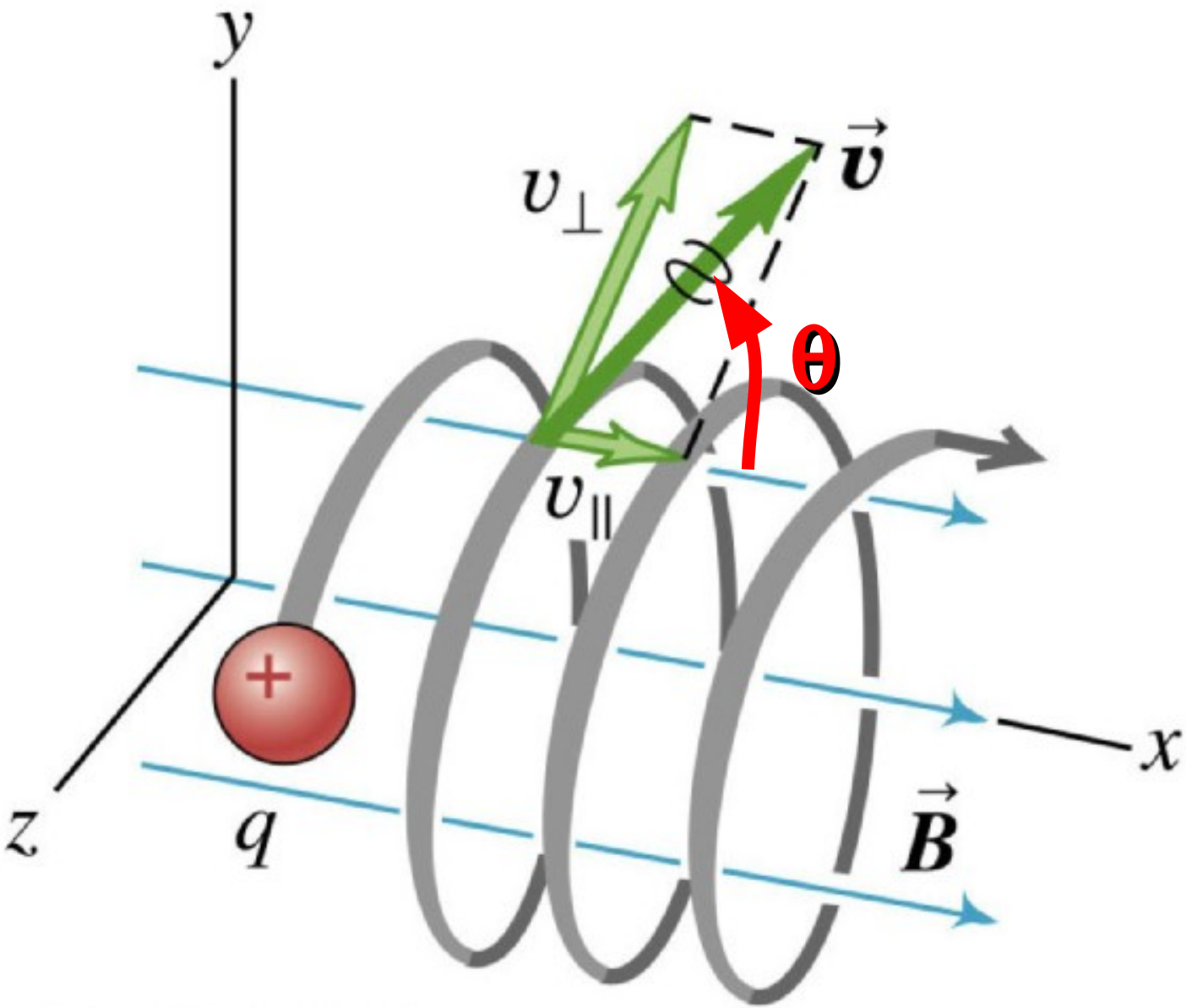

Cosmic-Ray Anisotropy =

large-scale **small-scales**

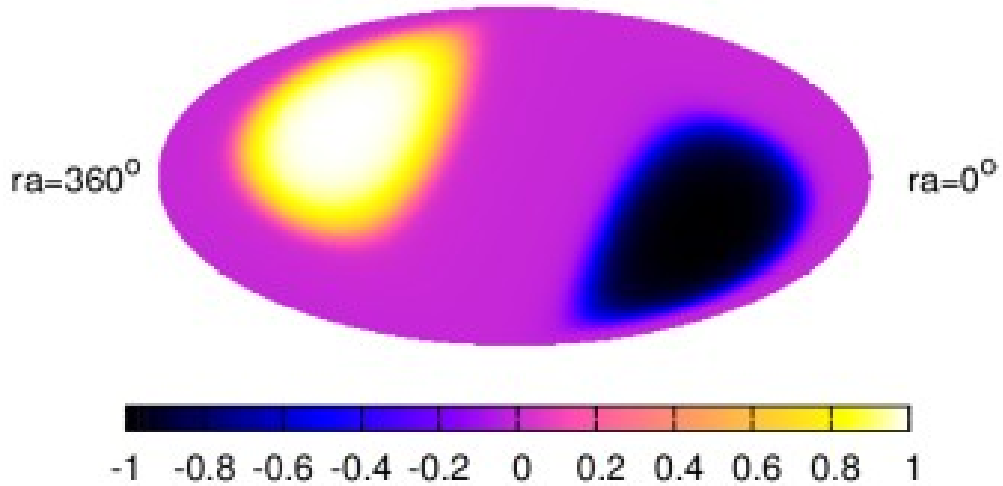

+

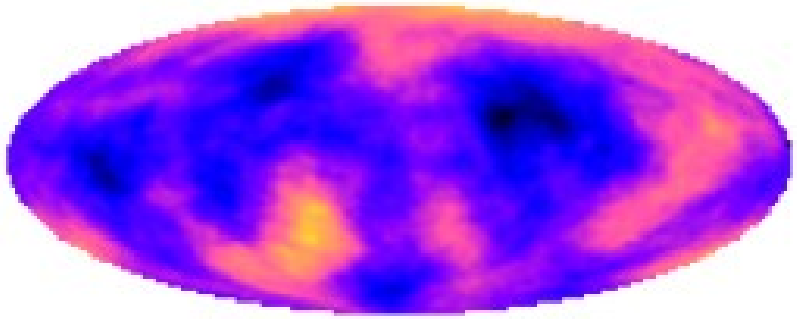

→ In the direction of field lines
→ Amplitude

→ **<u>SHAPE:</u>** not a dipole in general

HAWC:

SSA (l>3):

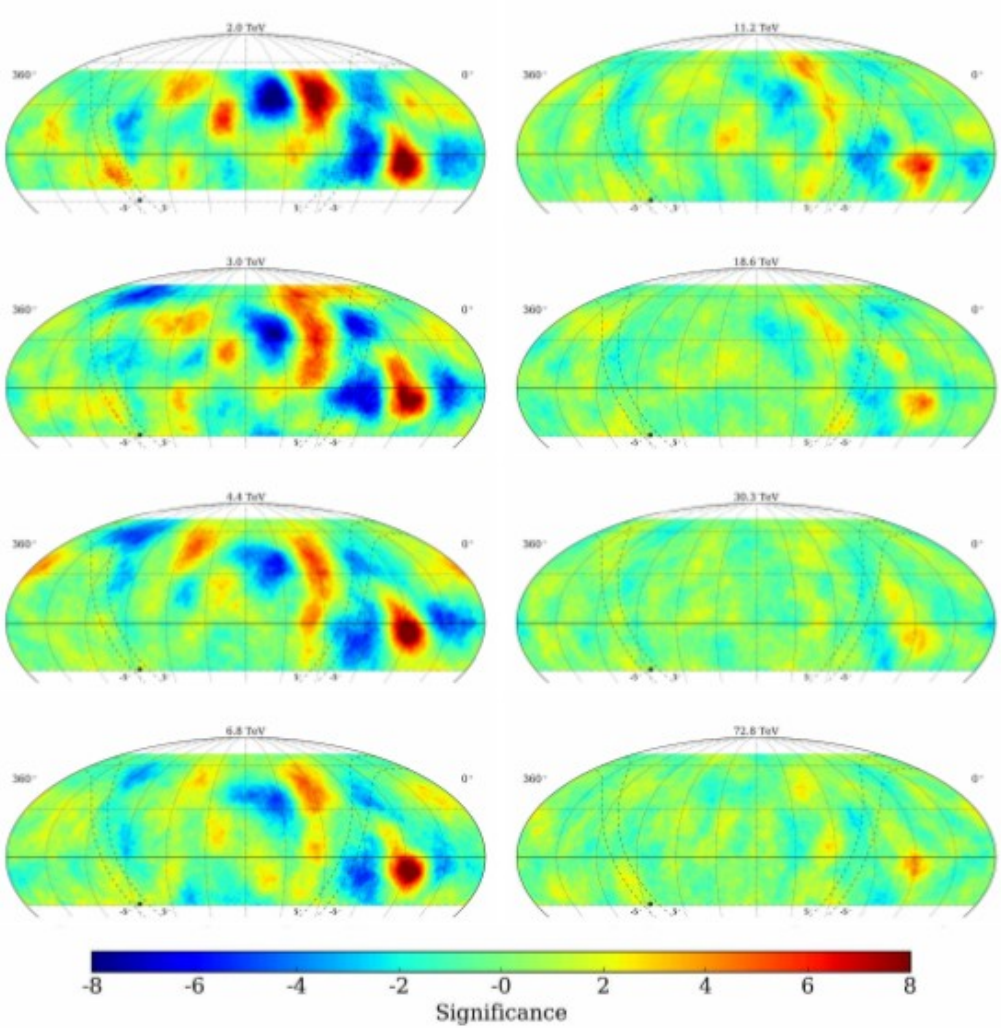

LSA:

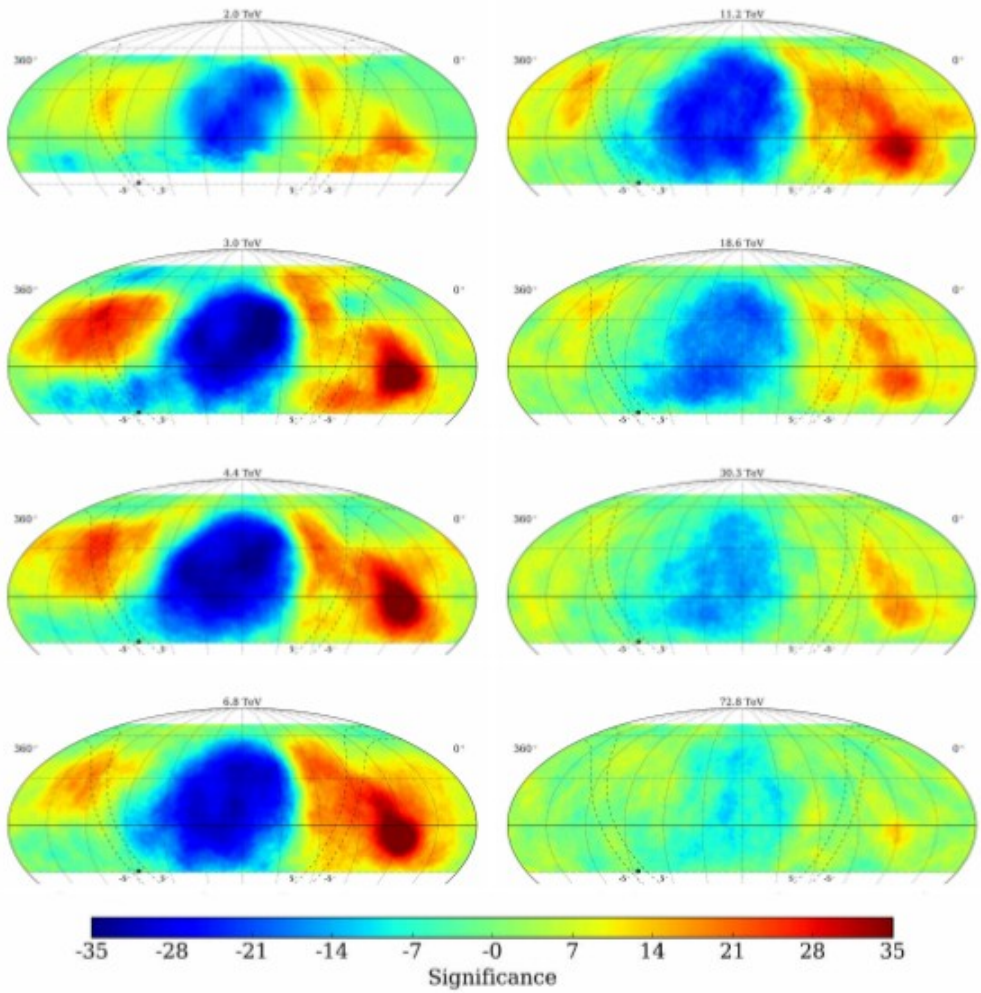

Observations (IceCube, IceTop)

Aartsen et al. (2013)

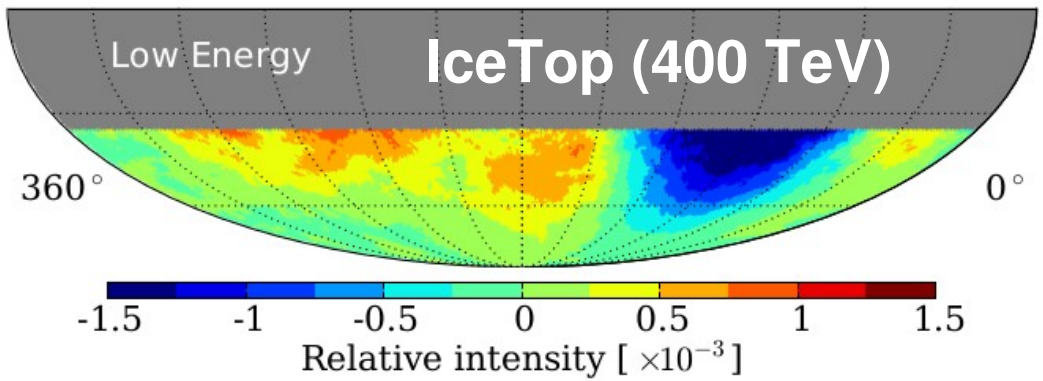

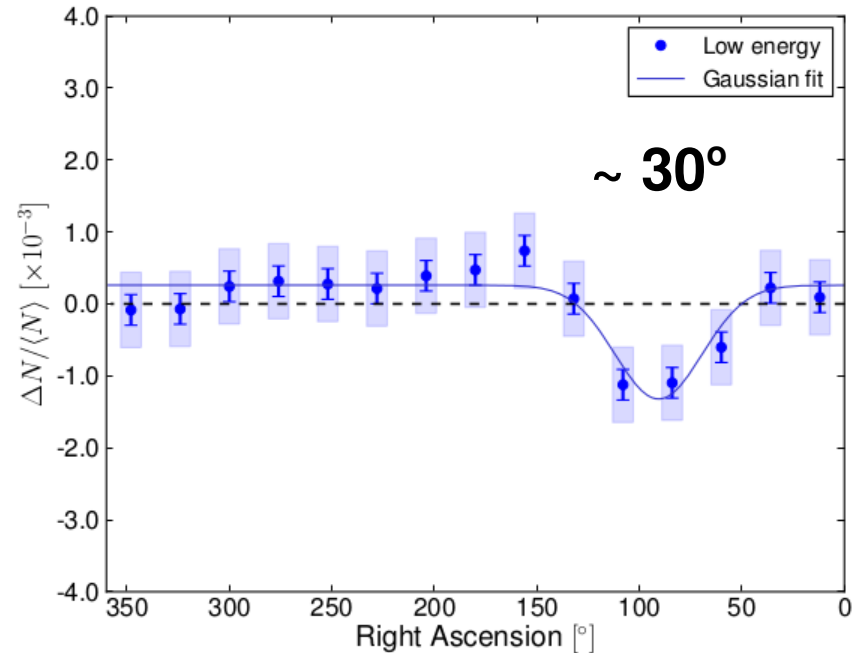

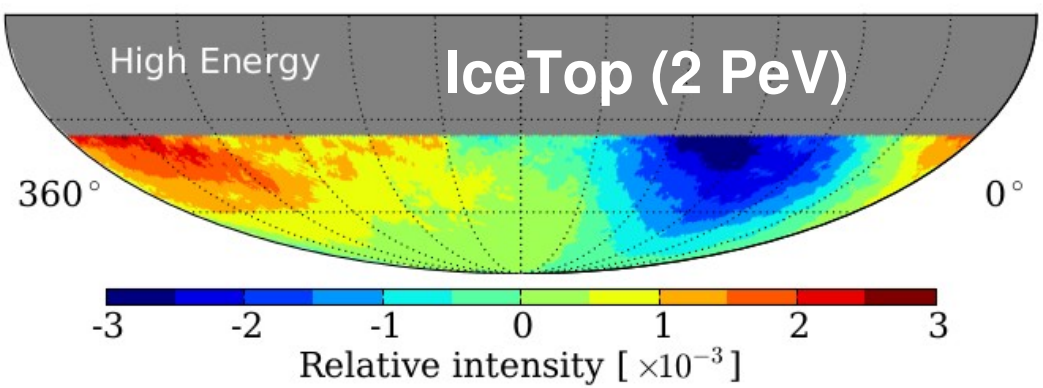

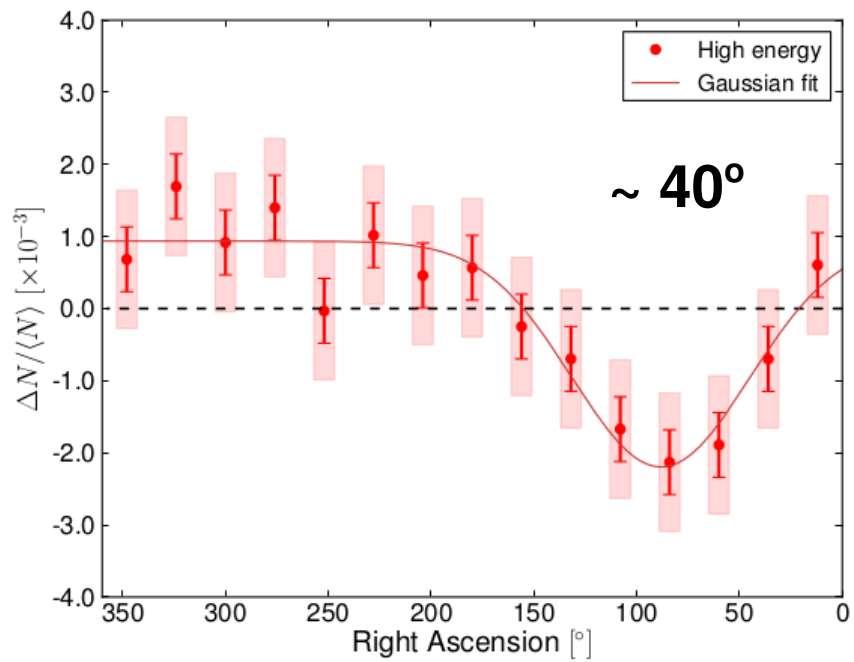

CR Anisotropy : Probe of turbulence

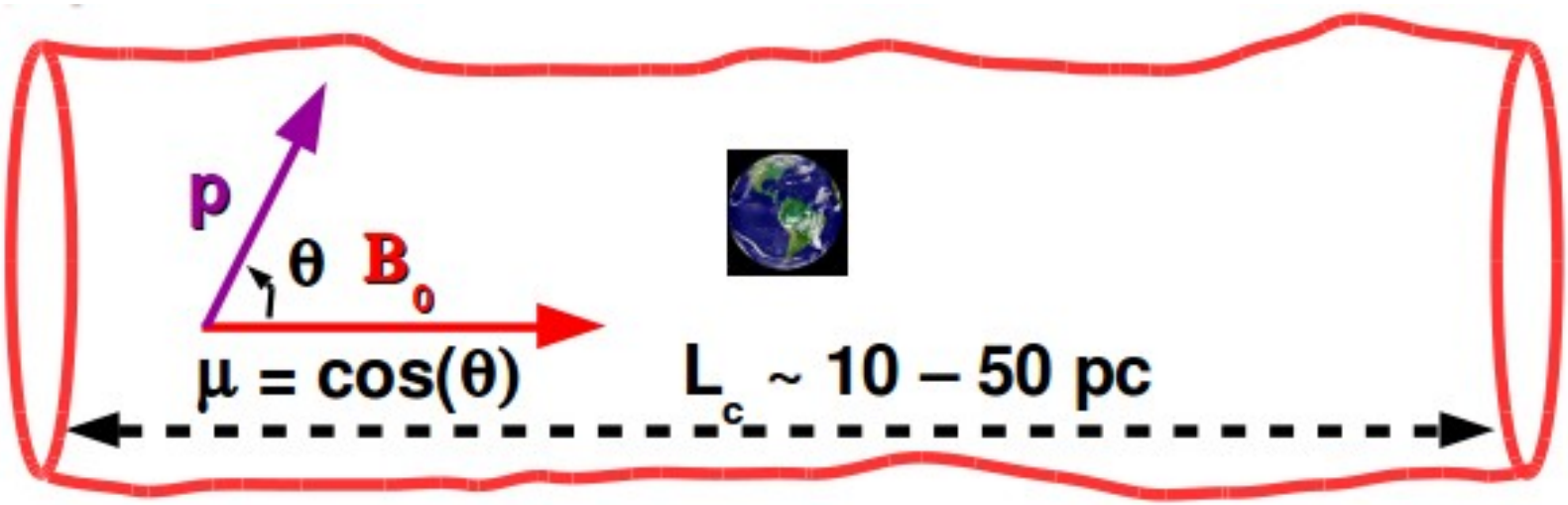

$$\mu v \frac{\partial f}{\partial x} = \frac{\partial}{\partial \mu}\left(D_{\mu\mu} \frac{\partial f}{\partial \mu} \right)$$

Pitch-angle diffusion

(gyrophase-averaged)

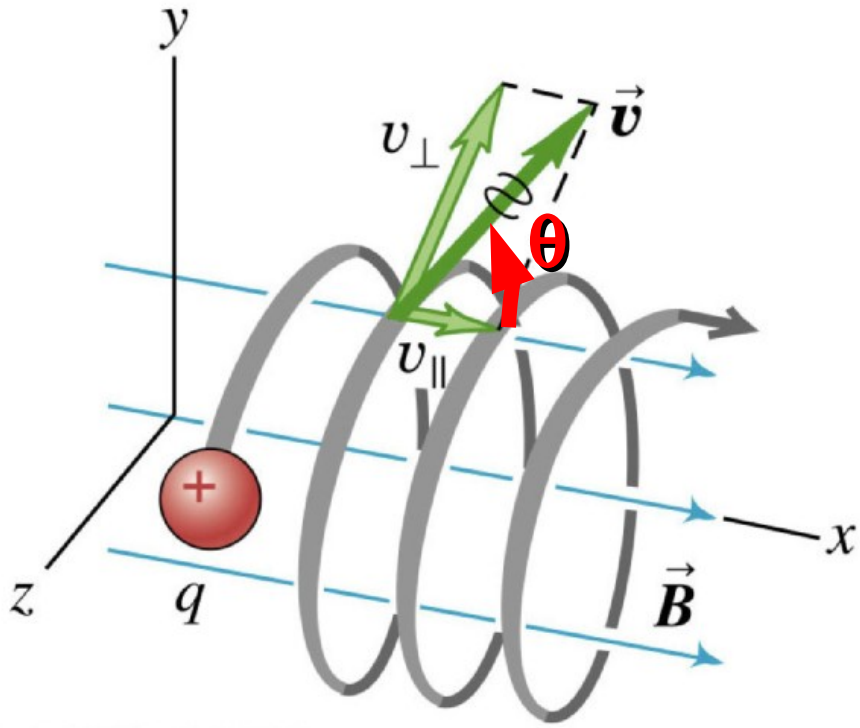

CR Anisotropy : Probe of turbulence

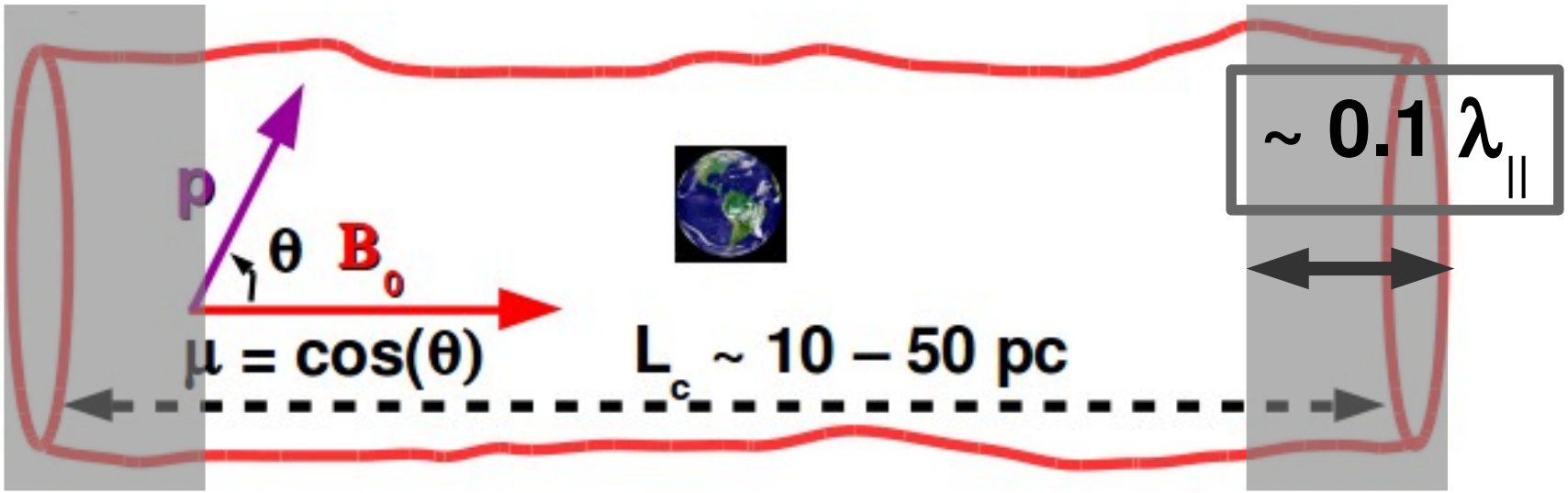

$$\mu v \frac{\partial f}{\partial x} = \frac{\partial}{\partial \mu}\left(D_{\mu\mu}\frac{\partial f}{\partial \mu}\right)$$

$$\int_0^{\mu} \mathrm{d}\mu' \, \frac{1-\mu'^2}{D_{\mu'\mu'}}$$

α

=> $f(x,\mu) = \sum_i a_i e^{\Lambda_i x/v} Q_i(\mu) + a_{\rm diff}\left[x + g(\mu)\right]$ + f_0

if $\exp\left(-\Lambda_1 d/v\right) \ll 1$

(« boundary layer »)

NOT $1 - \mu^2$ **in general !**

GG & Kirk, ApJ 835, 258 (2017), arXiv:1610.06134

Alfven (and Slow) modes

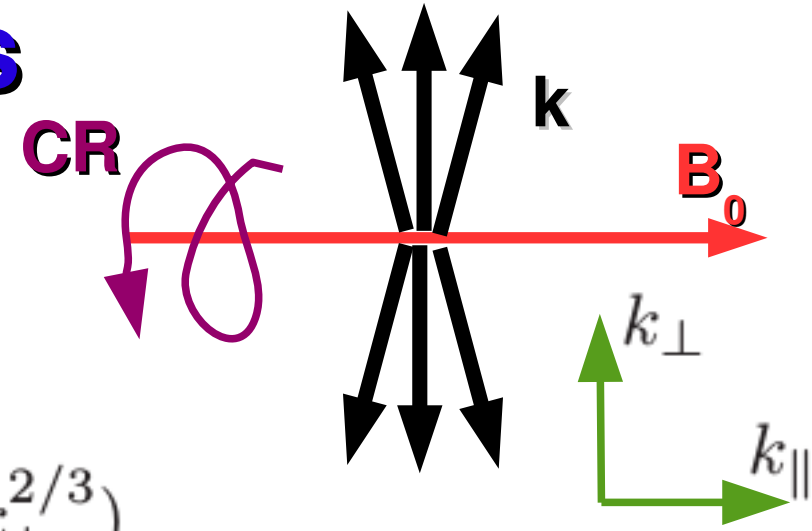

Goldreich & Sridhar (1995)

$$|k_\parallel| \lesssim |k_\perp|^{2/3} l^{-1/3}$$

(1) $$\mathcal{I}_{\mathrm{A,S}} = \mathcal{I}_{1,\mathrm{A,S}} \propto k_\perp^{-10/3} h(k_\parallel l^{1/3}/k_\perp^{2/3})$$

where $h(y) = 1$ if $|y| < 1$, and $h = 0$ otherwise (see Chandran (2000))

(2) MHD simulations of Cho & Lazarian (2002) :

$$\mathcal{I}_{\mathrm{A,S}} = \mathcal{I}_{2,\mathrm{A,S}} \propto k_\perp^{-10/3} \exp(-k_\parallel l^{1/3}/k_\perp^{2/3})$$

Fast magnetosonic modes

MHD simulations of Cho & Lazarian (2002) :

Isotropic with $\mathcal{I}_{\mathrm{M}}(\mathbf{k}) \propto k^{-3/2}$

Pitch-angle diffusion coefficient

$$D_{\mu\mu} = \Omega^2 \left(1-\mu^2\right) \int \mathrm{d}^3k \sum_{n=-\infty}^{\infty} \left(\frac{n^2 J_{\mathrm{n}}^2(z)}{z^2} \mathcal{I}_{\mathrm{A}}(\mathbf{k}) + \frac{k_{\parallel}^2 J_{\mathrm{n}}'^2(z)}{k^2} \mathcal{I}_{\mathrm{S,F}}(\mathbf{k}) \right) \times R_{\mathrm{n}}(k_{\parallel} v_{\parallel} - \omega + n\Omega) \ ,$$

where $\mathcal{I}_{\mathrm{A,S,F}}$ respectively correspond to the normalized energy spectra of the Alfvén, slow and fast modes.

$z = k_{\perp} l \varepsilon \sqrt{1-\mu^2}$, and Ω is the Larmor frequency.

$\varepsilon = v/(l\Omega) = r_{\mathrm{L}}/l$

(R. Keppens)

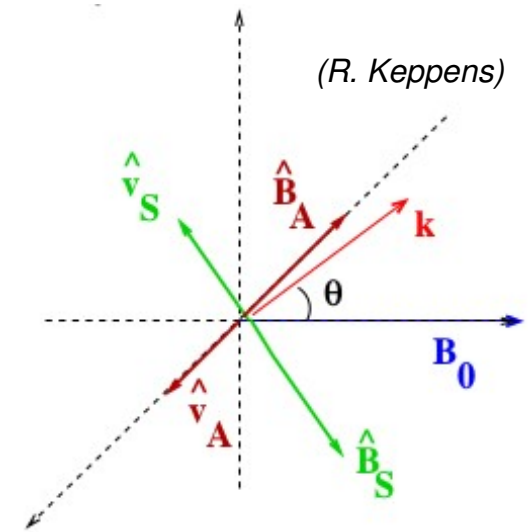

Resonance functions (RF)

(1) NARROW: RF dominated by Lagrangian correlation time (τ_w)

Chandran (2000)

$$R_{n,1}(k_\parallel v_\parallel - \omega + n\Omega) = \frac{\tau_w^{-1}}{(k_\parallel v_\parallel - \omega + n\Omega)^2 + \tau_w^{-2}}$$

Lagr. corr. time for strong aniso. incompr. MHD turb. → $\tau_{A,S} = l^{1/3}/(v_A k_\perp^{2/3})$

$$\tau_F = l/(v_A \tilde{k}^{1/2}) \qquad \tilde{k} = kl$$

(2) BROAD: Conservation of the adiabatic invariant $v_\perp^2/B$

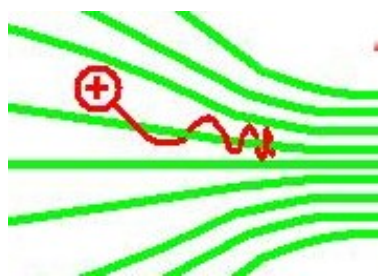

Yan & Lazarian (2008)

$$\delta\mathcal{M}_A = \sqrt{\langle \delta B_\parallel^2 \rangle / B_0^2}$$

$$R_{n,2}(k_\parallel v_\parallel - \omega + n\Omega) = \frac{\sqrt{\pi}}{k_\parallel v_\perp \delta\mathcal{M}_A^{1/2}} \exp\left(-\frac{(k_\parallel v_\parallel - \omega + n\Omega)^2}{k_\parallel^2 v_\perp^2 \delta\mathcal{M}_A}\right)$$

Case E : Fast modes & Narrow RF

No visible dependence of the *shape* on CR energy $\varepsilon = v/(l\Omega) = r_{\rm L}/l$

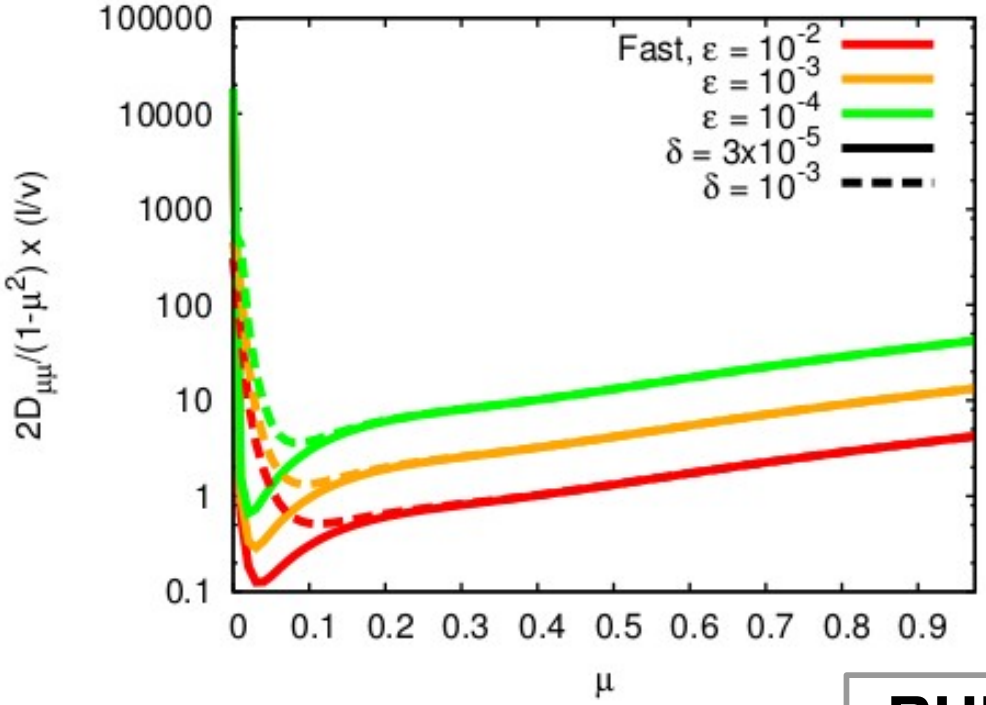

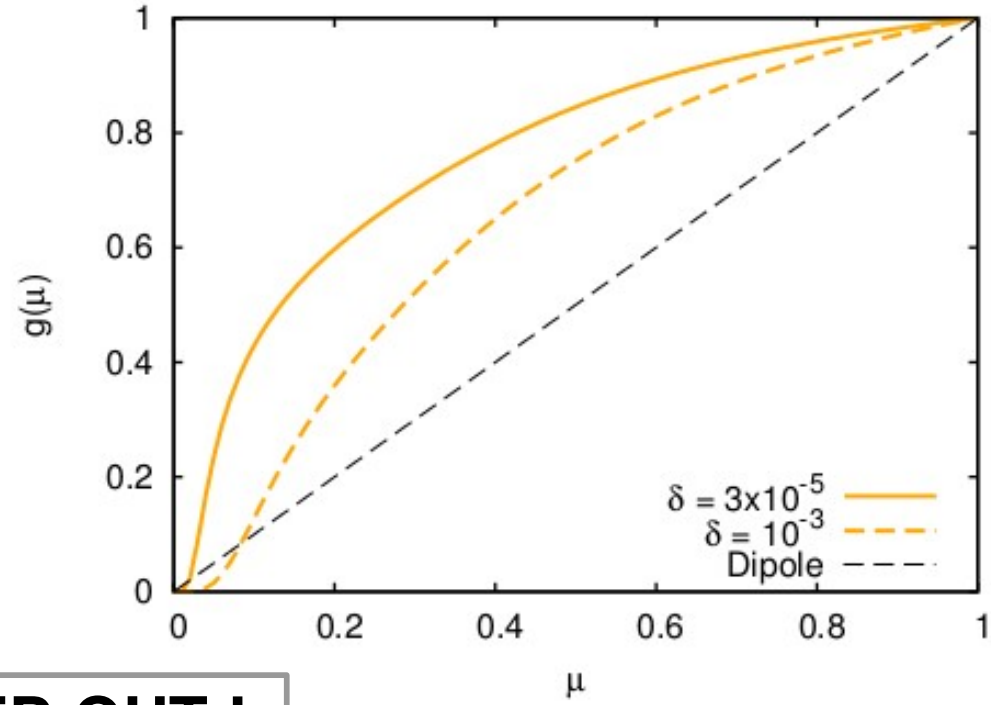

RULED OUT !

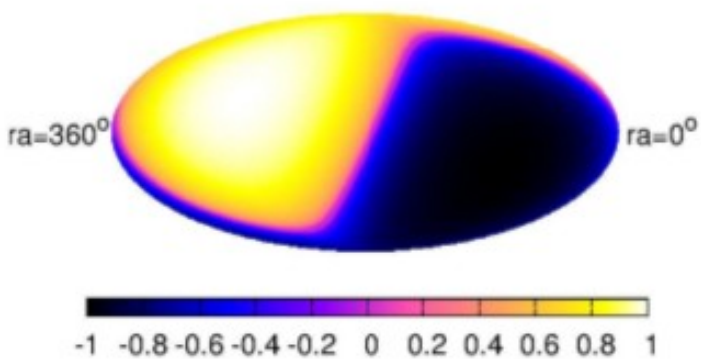

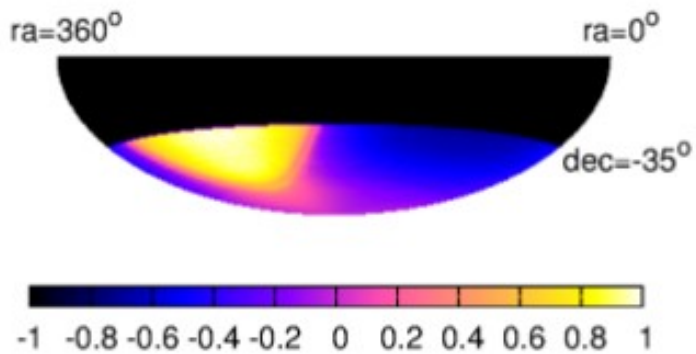

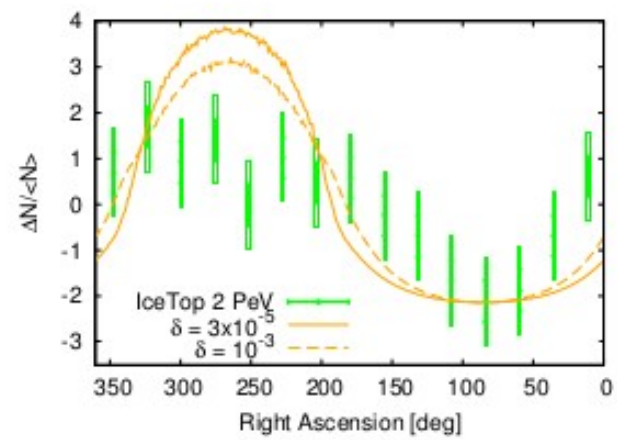

In general: Anisotropy is too wide with the narrow RF.

Case C : GS – Heaviside & Broad RF

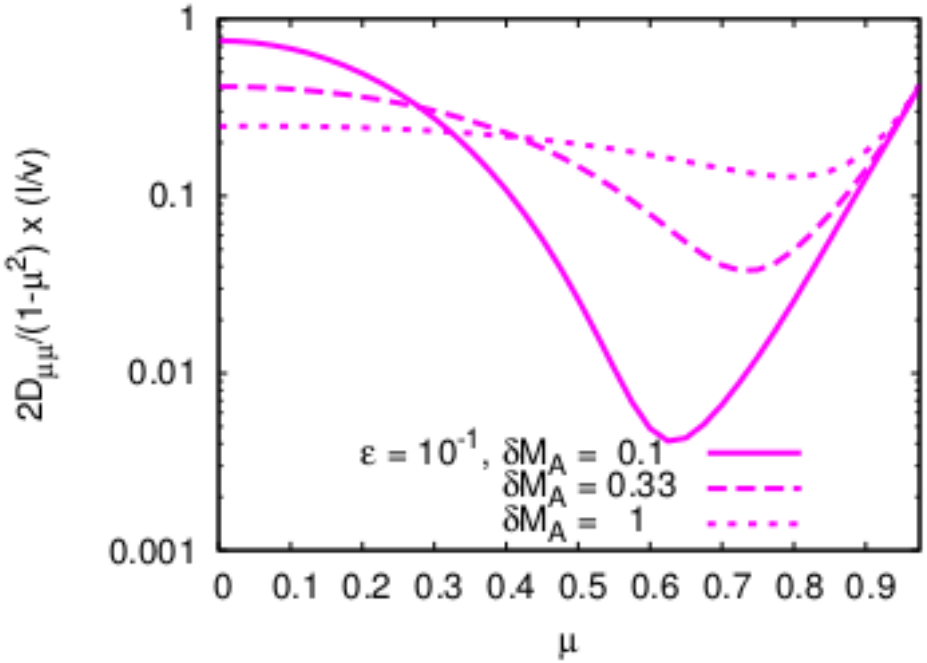

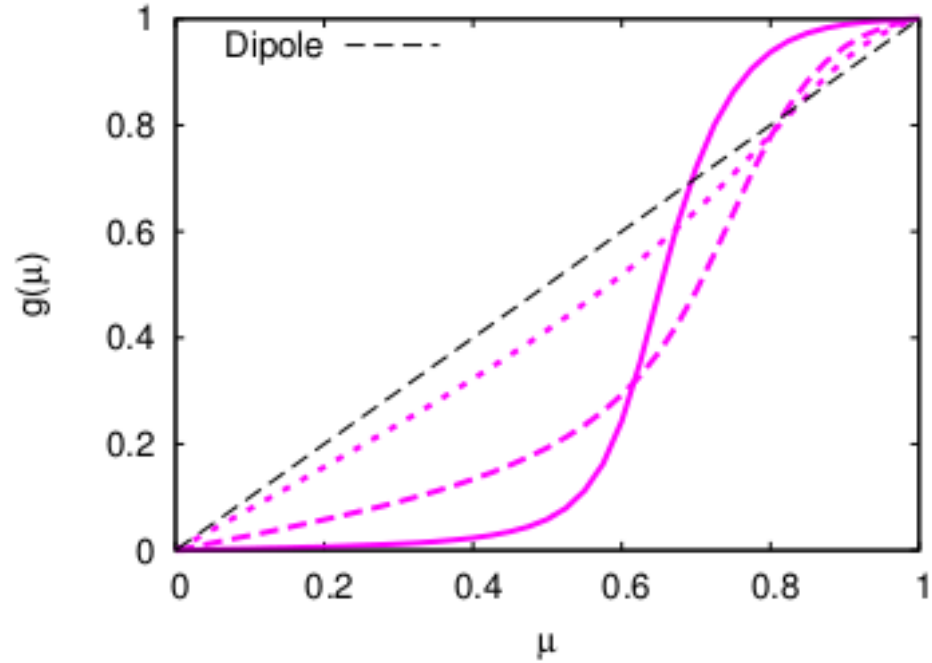

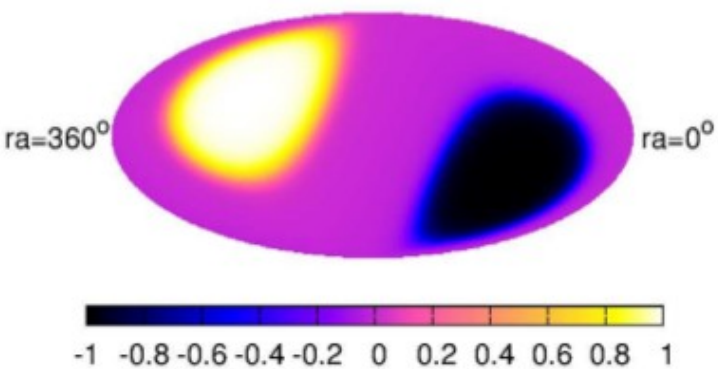

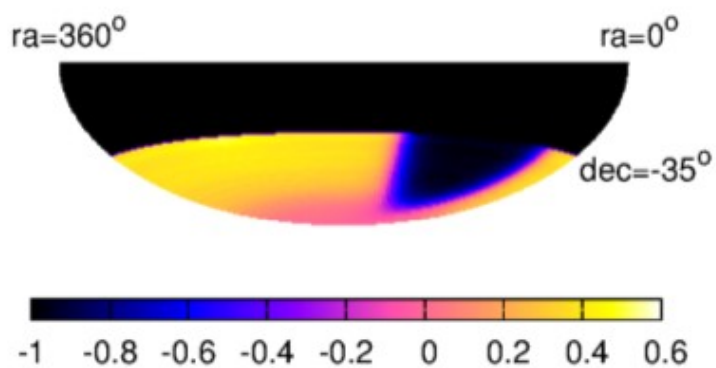

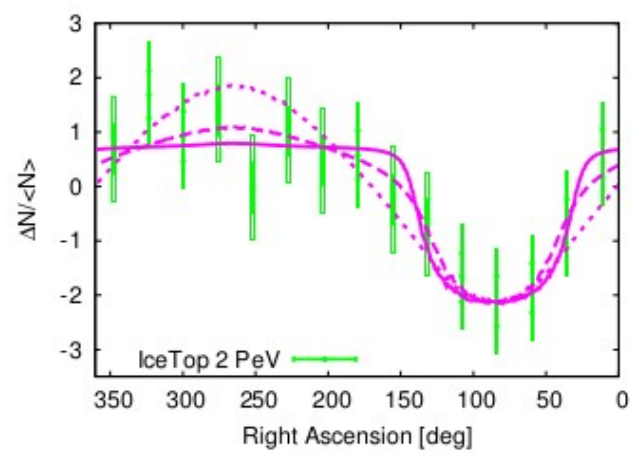

Case D : GS – Exponential & Broad RF

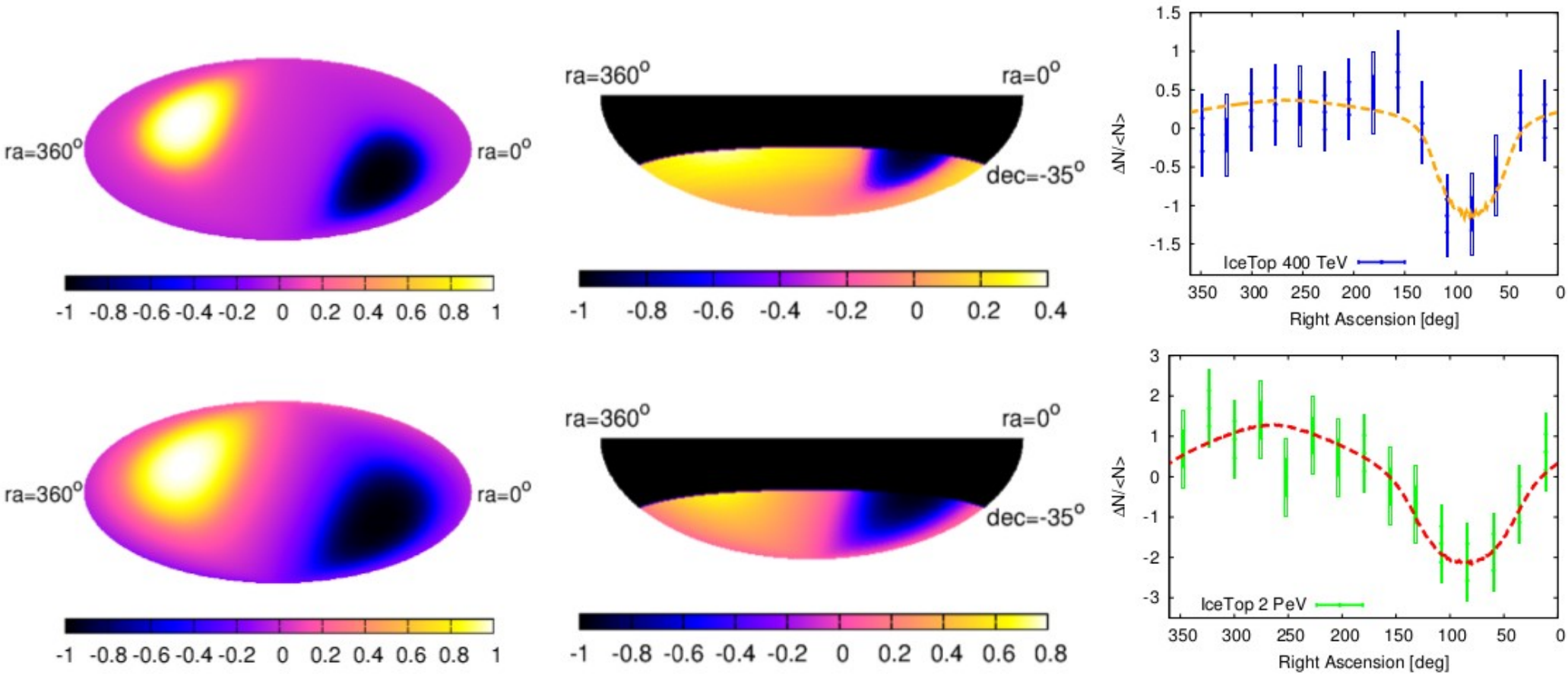

Can fit well the 400 TeV and the 2 PeV data !

Energy-dependence reproduced for fixed turbulence parameters

Case F : Fast modes & Broad RF

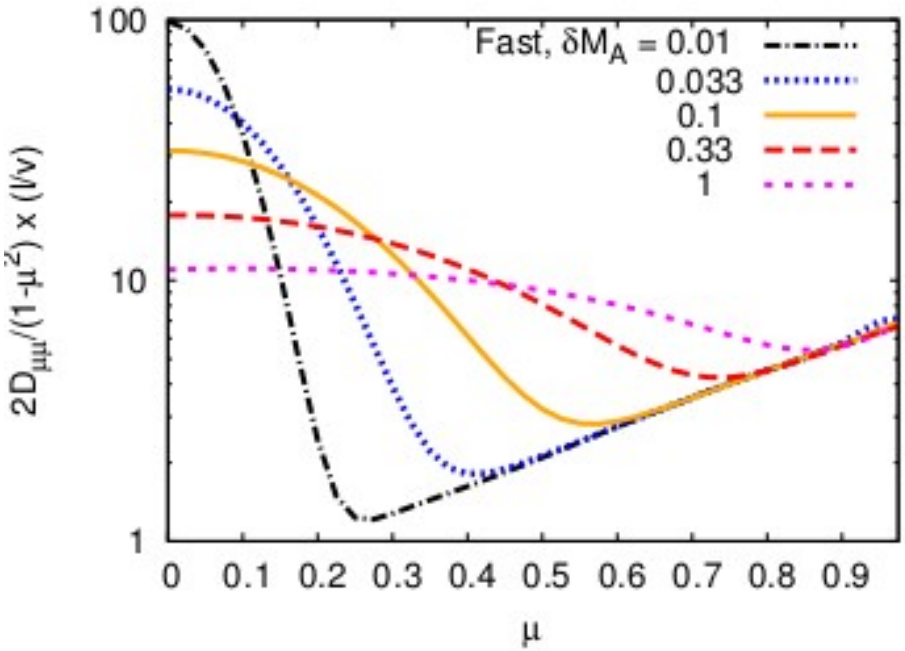

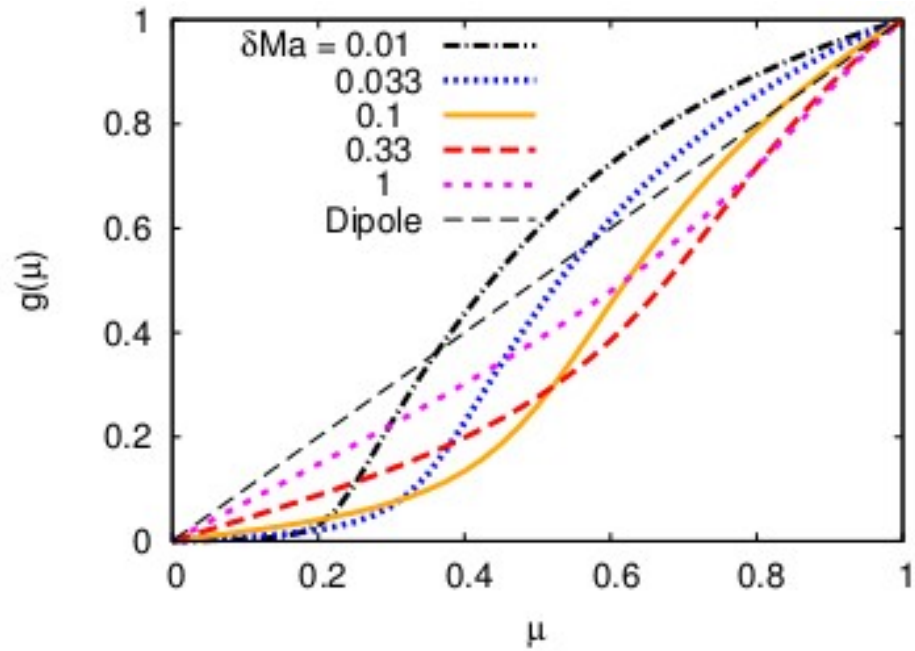

Can **fit the 2 PeV data** ! →

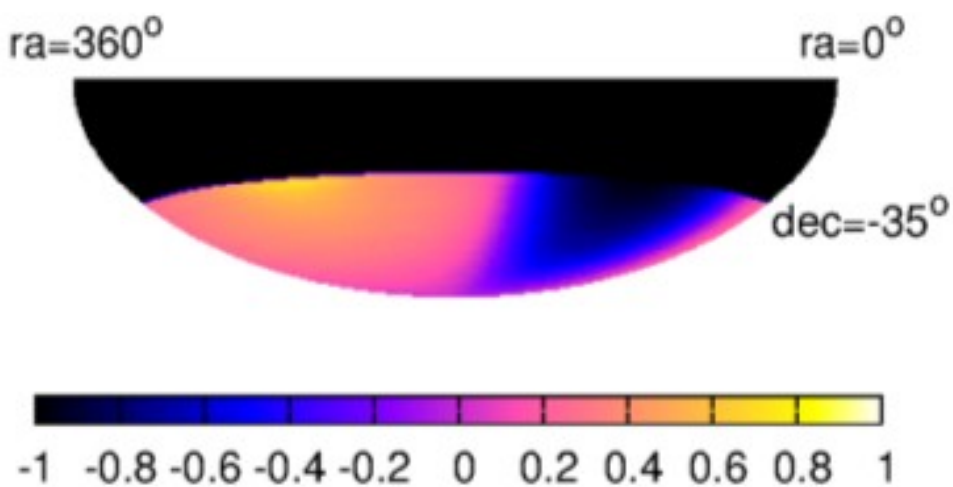

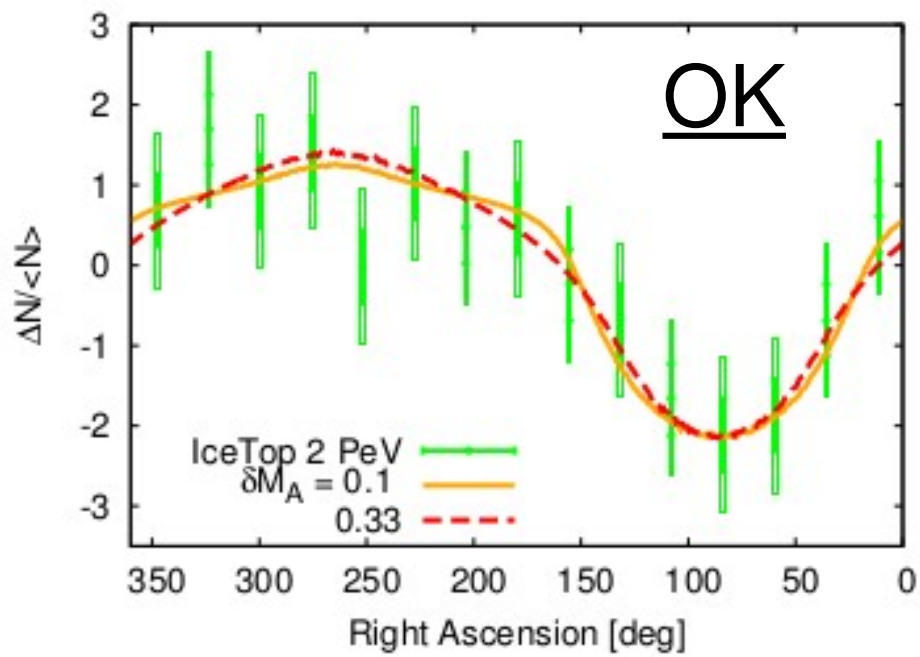

LS CRA – Summary :

Large-scale CR Anisotropy = NEW Probe of

(i) local <u>ISMFs</u> (Modes and their anisotropy in k-space)

(ii) local <u>CR transport properties</u>

The existing data already places constraints !

→ Flattening in directions perpendicular to field lines,

→ Can fit the 2 PeV data with GS turbulence or fast modes with a moderately broad RF,

→ Constraints on res. functions : Narrow ones disfavoured,

→ Change in anisotropy shape with CR energy ?

- - -> |**k**|-dependent anisotropy in power spectrum ??

Small-scale anisotropies and local interstellar turbulence

GG & Sigl, Phys. Rev. Lett. 109, 071101 (2012),
arXiv:1111.2536

cf. Zhang et al. (2014) for a heliospheric origin at 1 – 10 TeV.

Diffusion approximation - Dipole

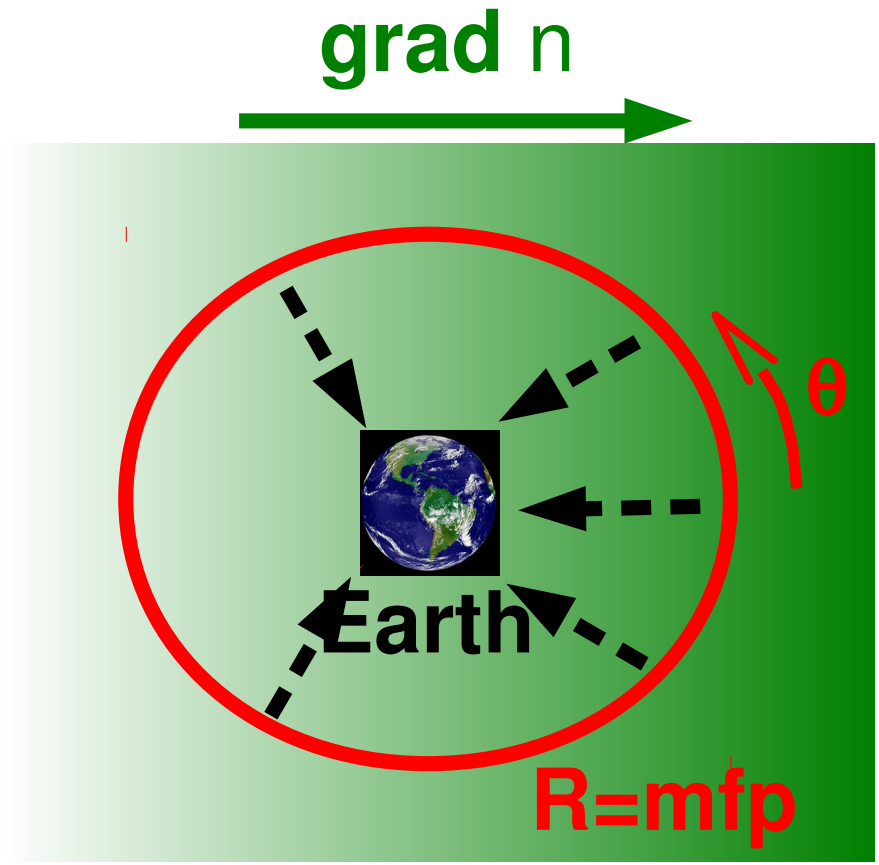

$$F = F_0 (1+\delta \cos \theta)$$

$$\boldsymbol{\delta}(p) \simeq -\frac{3}{c_0}\frac{\mathbf{j}}{n} = \frac{3D(p)}{c_0}\frac{\boldsymbol{\nabla} n}{n}$$

where $\mathbf{j}(\mathbf{r}, p) = -D(p)\boldsymbol{\nabla} n$ is the CR current

In reality :

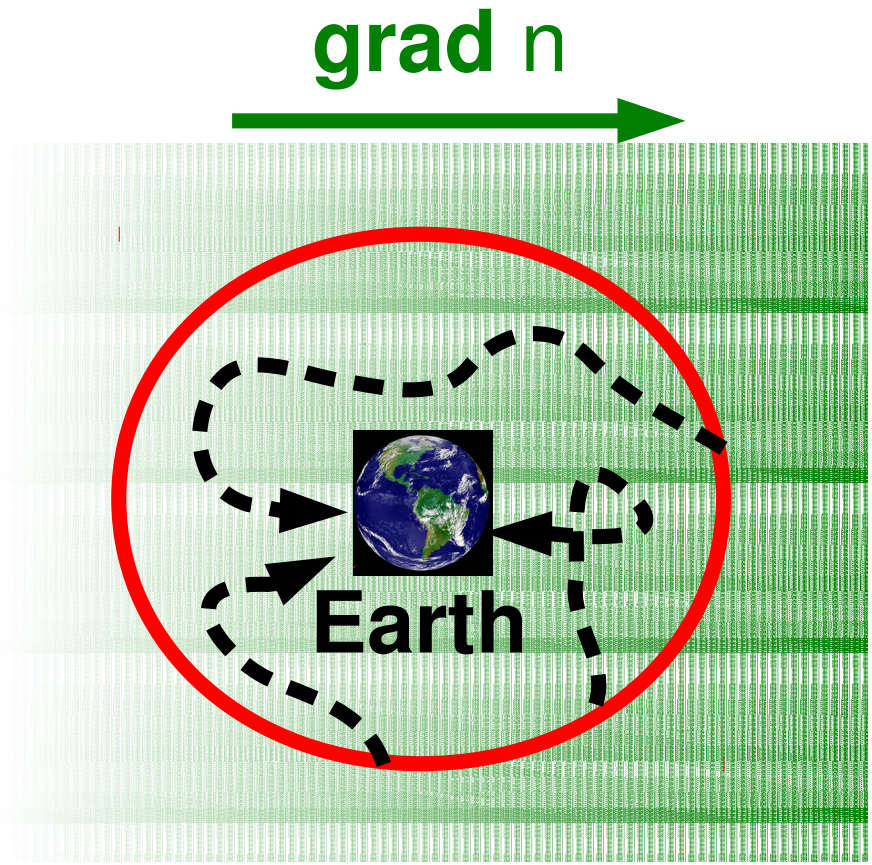

1) The local field does not vary significantly within experiment lifetime

2) The Earth is point-like (/r_L)

→ SSA due to the local configuration of the B field, within a CR MFP around Earth.

Numerical simulations

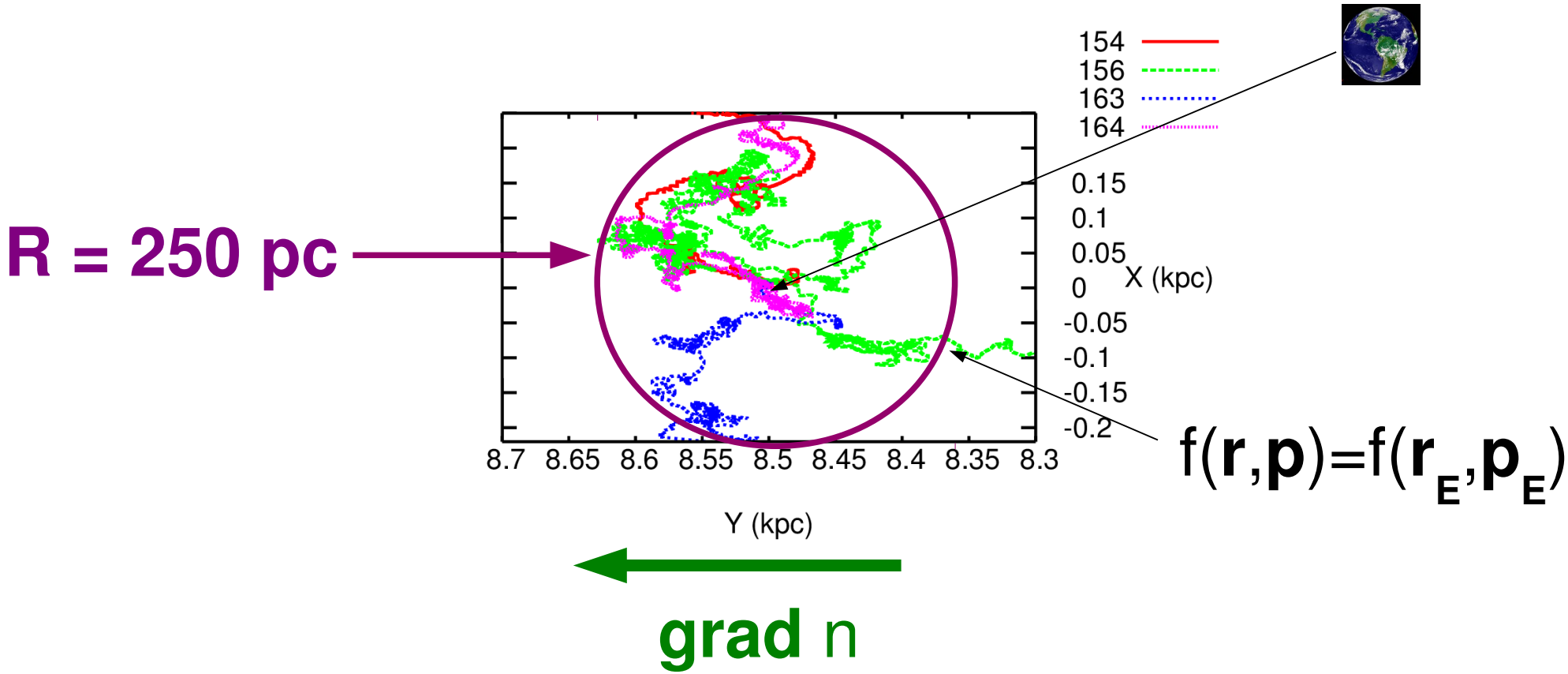

$$f(\mathbf{r},\mathbf{p}) \sim f_0(\mathbf{r},p)\,[1 + \mathbf{d}\,.\,\mathbf{p}/|\mathbf{p}|\,]$$

Large and Small scales

90° smoothing

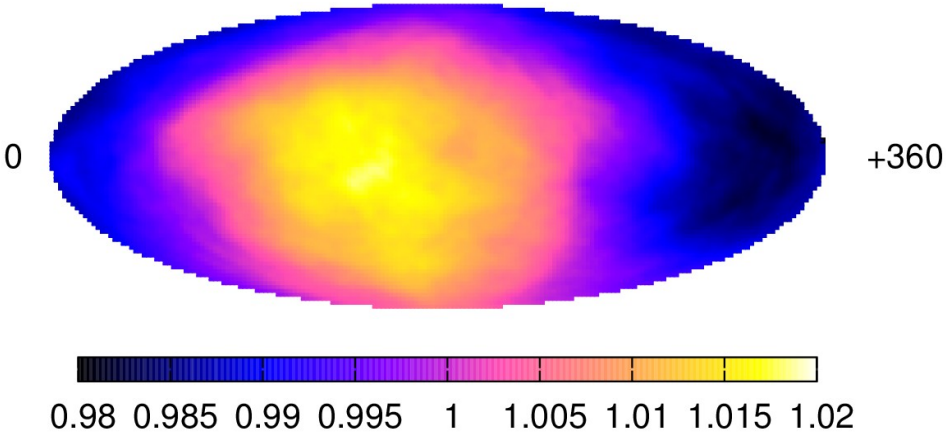

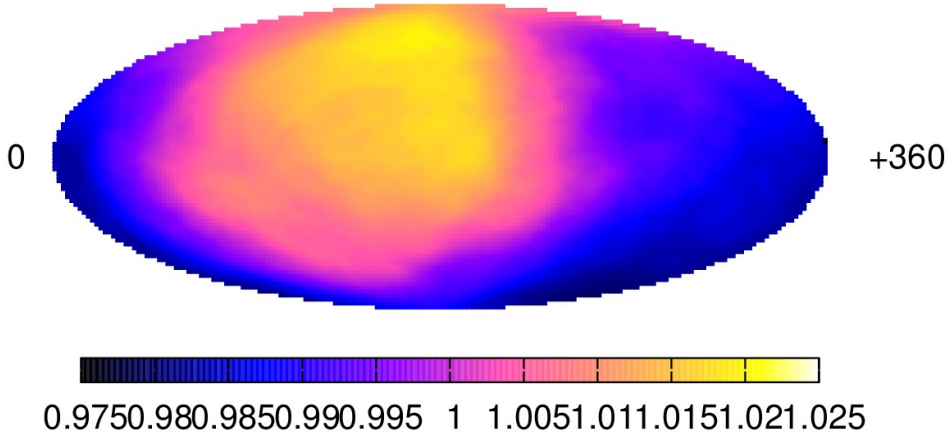

20° smoothing - Dipole

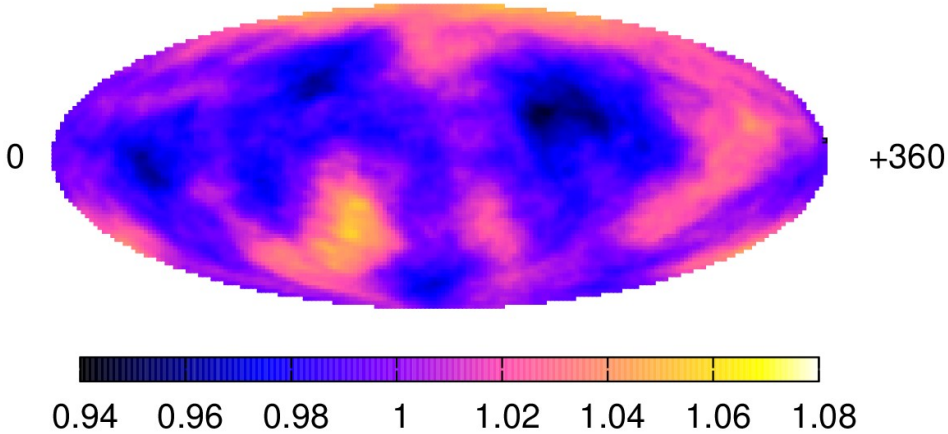

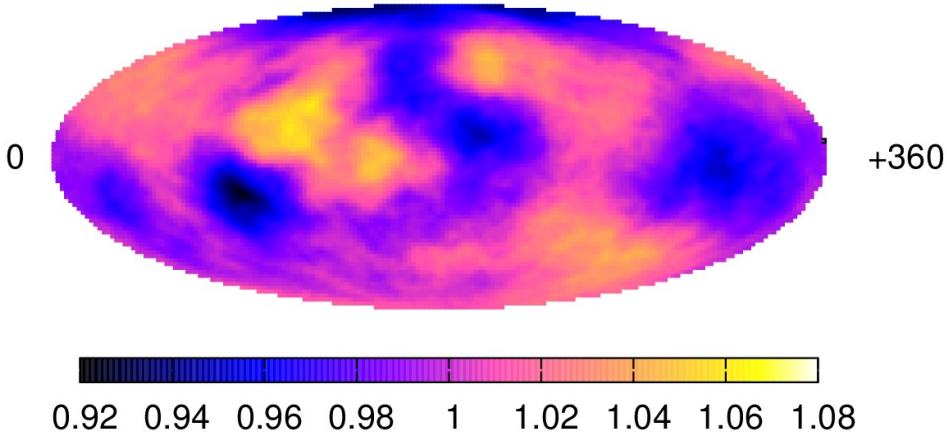

Numerical simulations down to 3 TeV

GG, In Prep. (2019) – *see also arXiv:1810.06396*

Individual CR trajectories

300 TeV, Kolmogorov, L_{max} = 150 pc, B_{rms} = 4 μG.

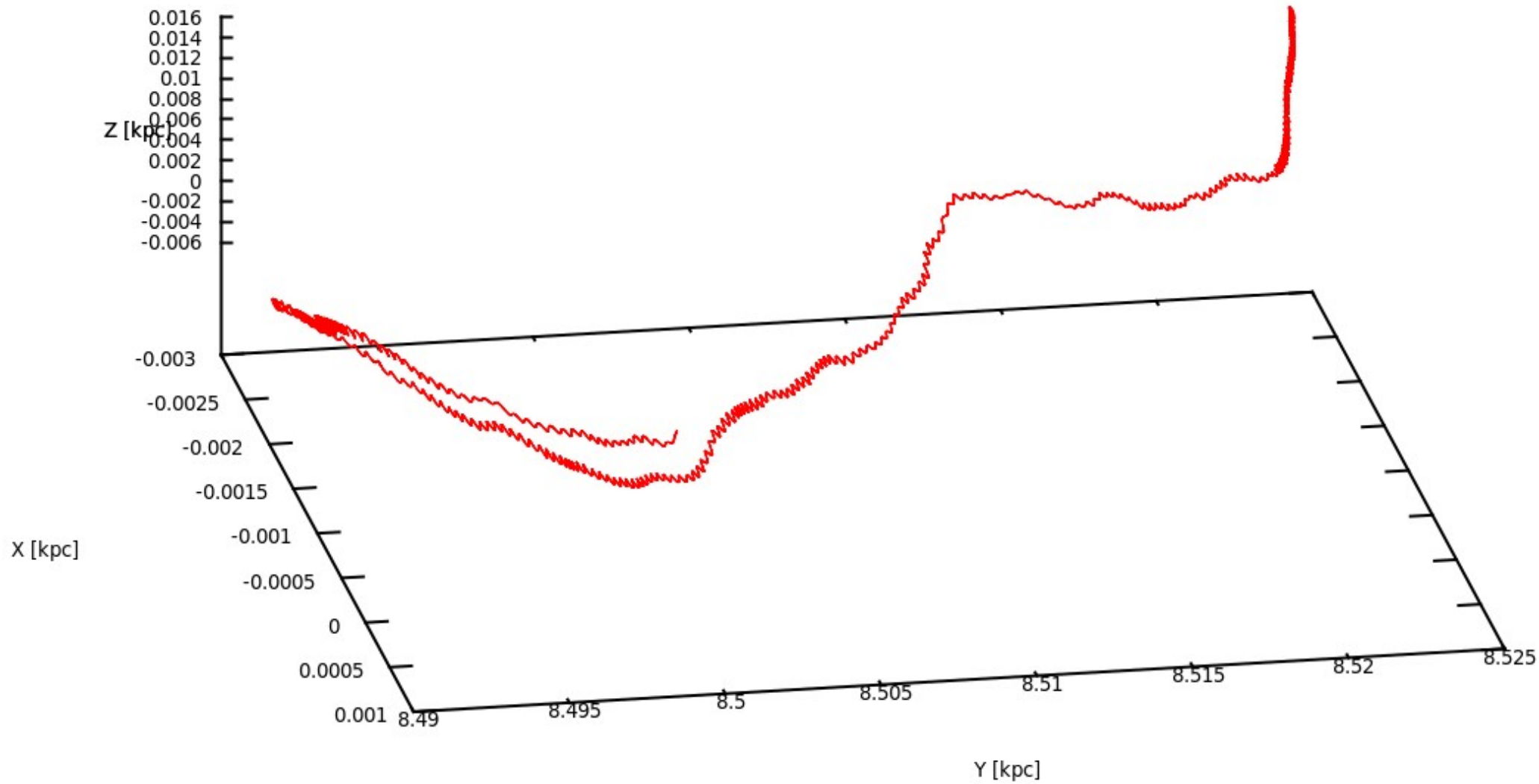

Individual CR trajectories

3 TeV, Kolmogorov, L_{max} = 150 pc, B_{rms} = 4 μG.

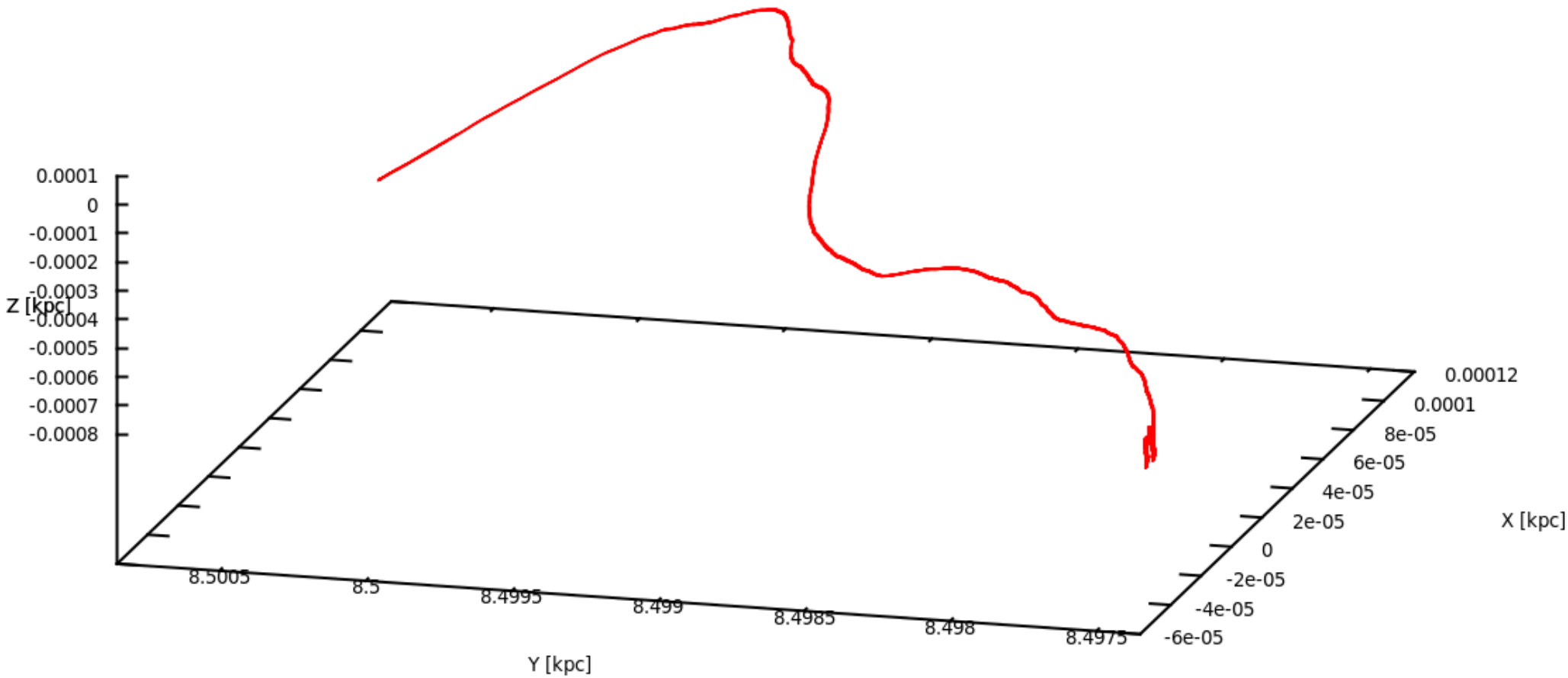

Numerical simulations (Config. 1)

E_{CR} = 3 PeV, Kolmogorov, L_{max} = 150 pc, B_{rms} = 4 μG.

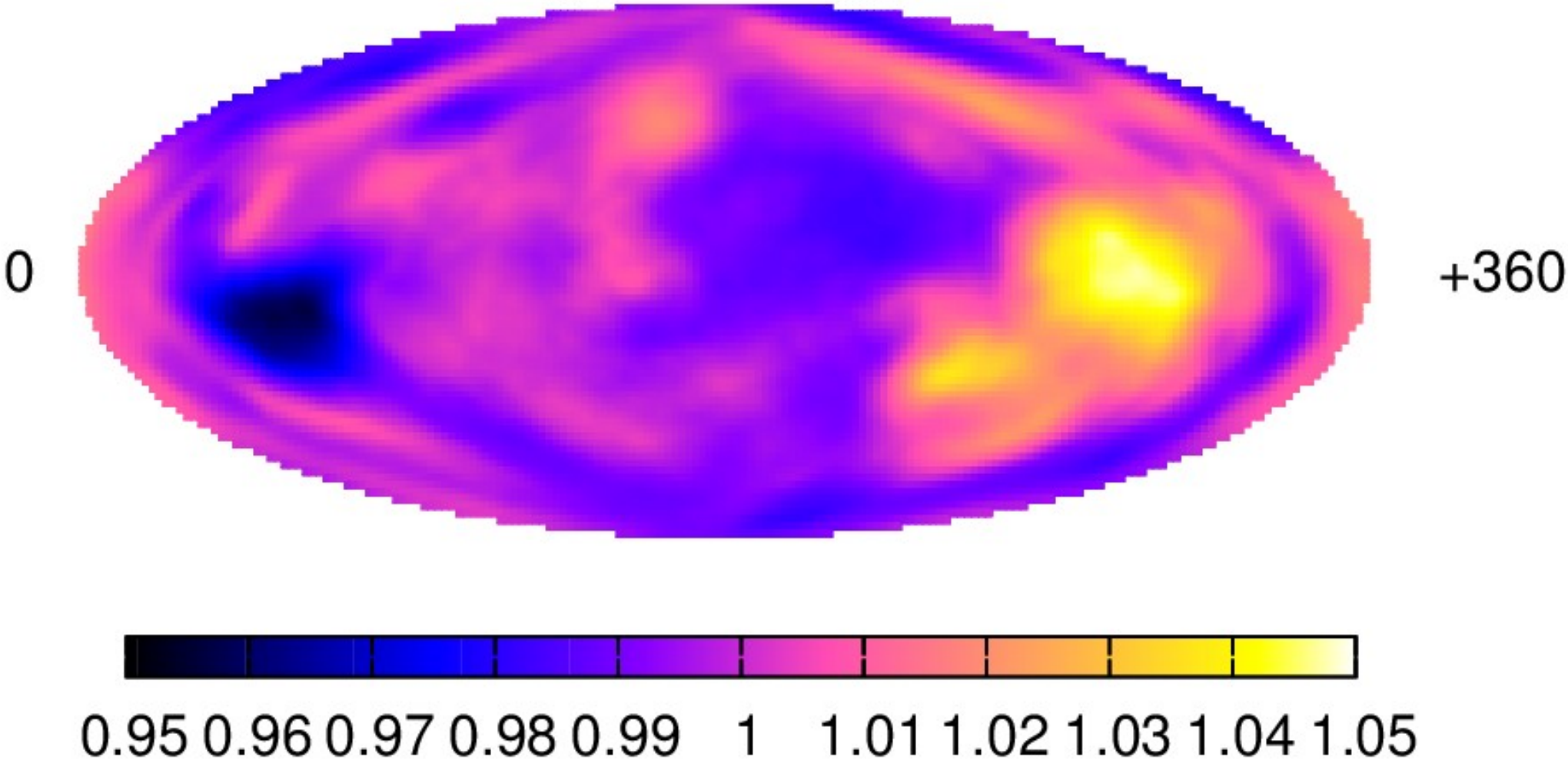

Numerical simulations (Config. 1)

E_{CR} = 1 PeV

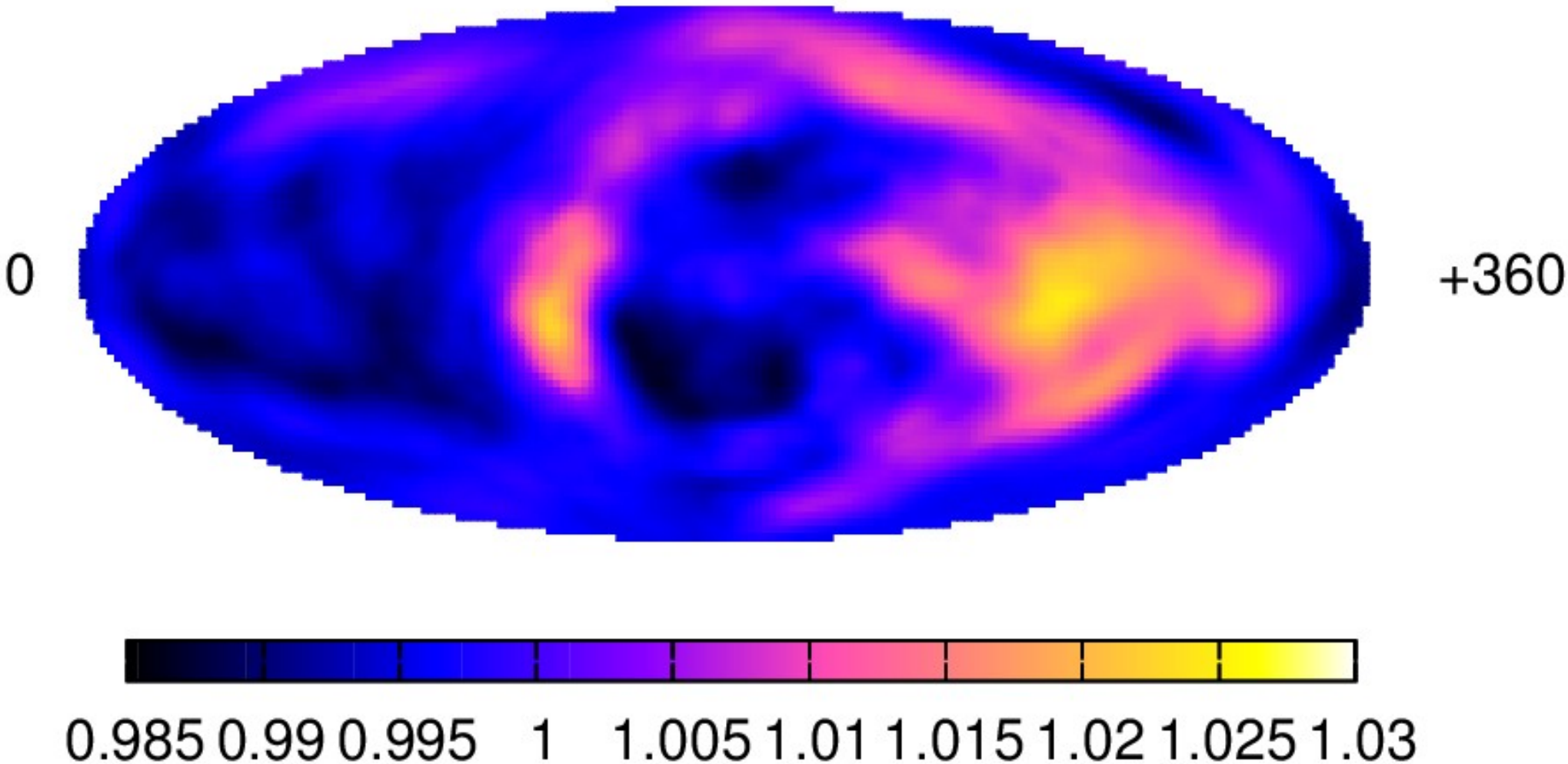

Numerical simulations (Config. 1)

E_{CR} = 300 TeV

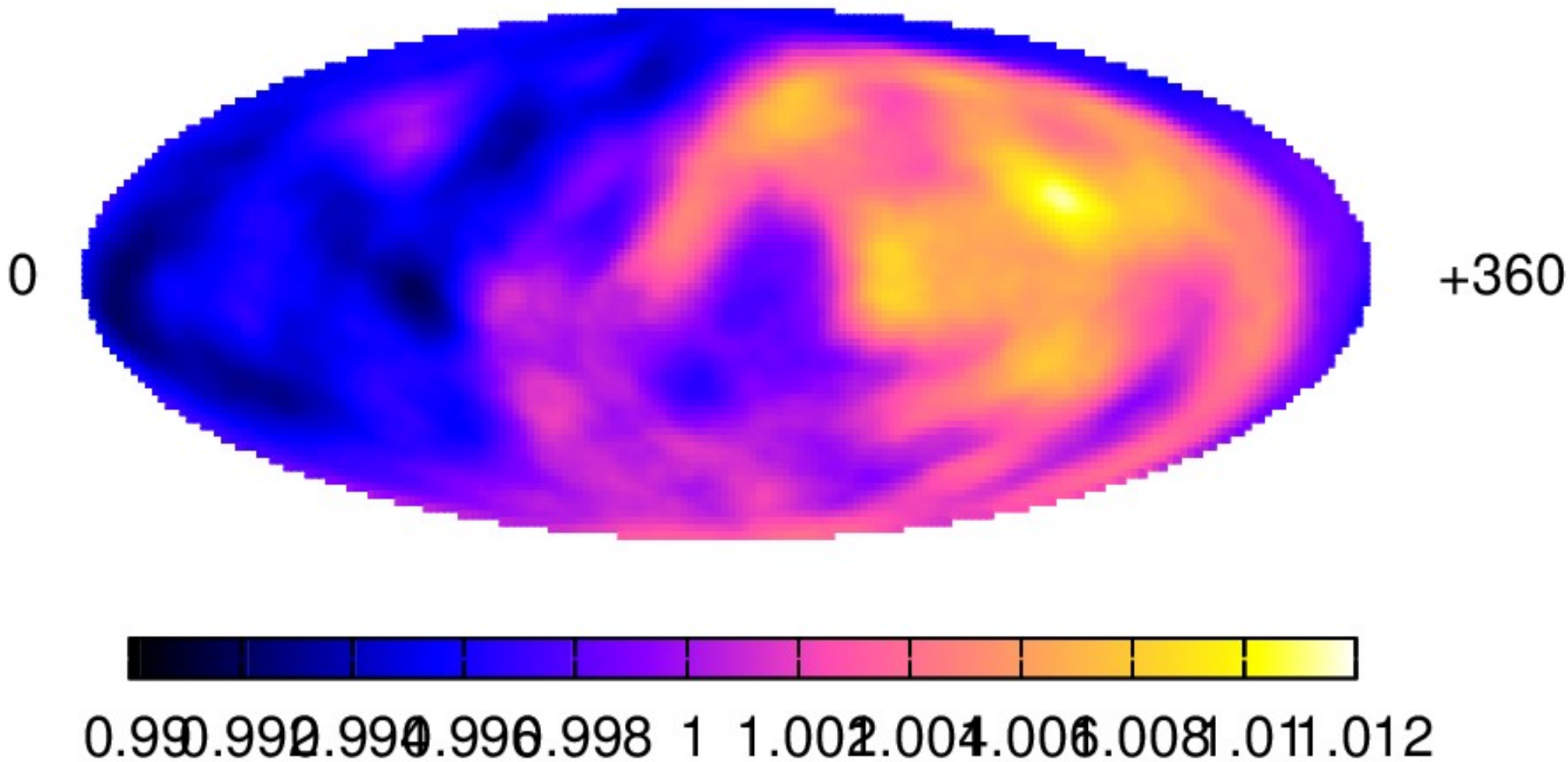

Numerical simulations (Config. 1)

E_{CR} = 100 TeV

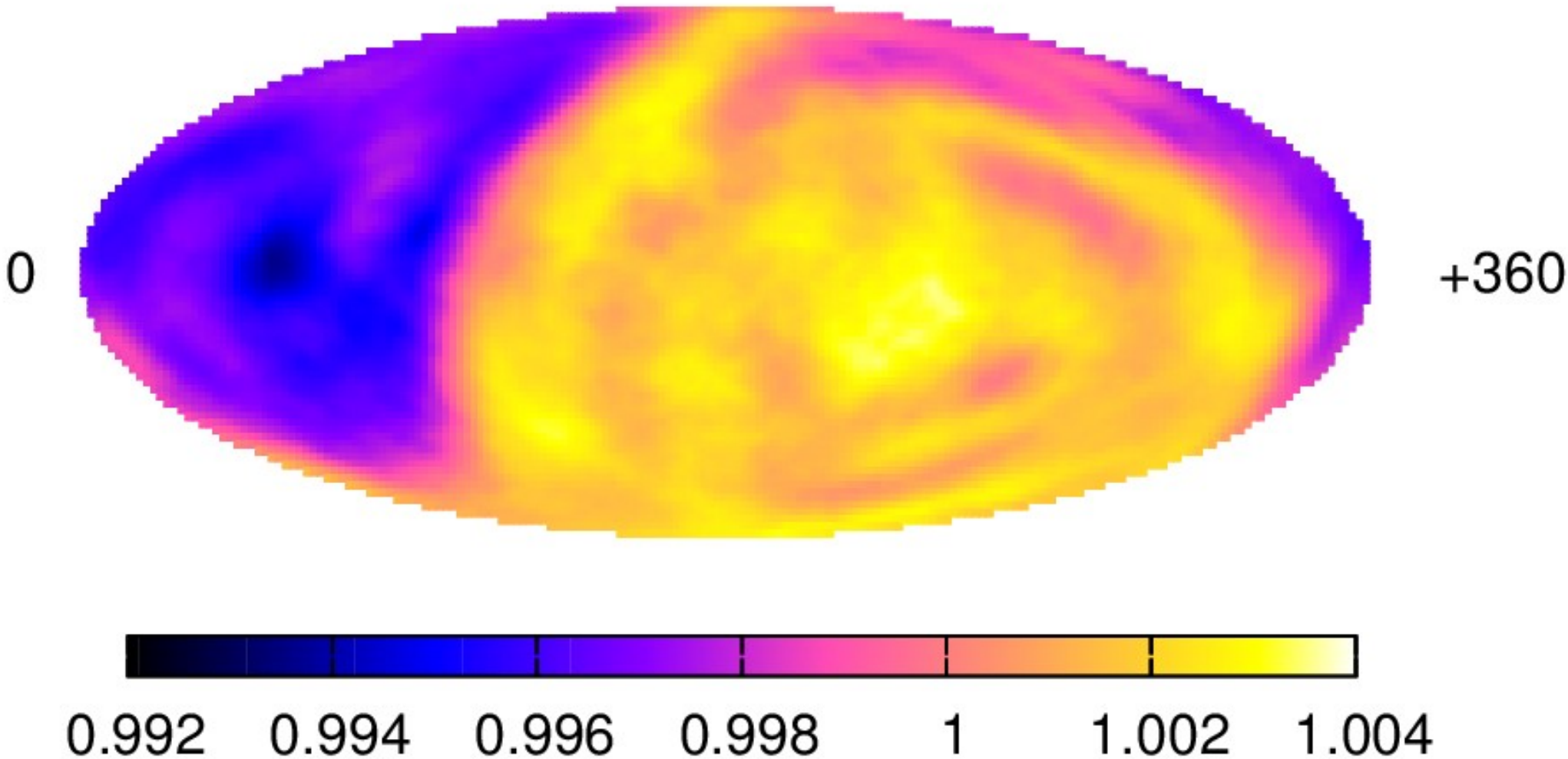

Numerical simulations (Config. 1)

E_{CR} = 30 TeV

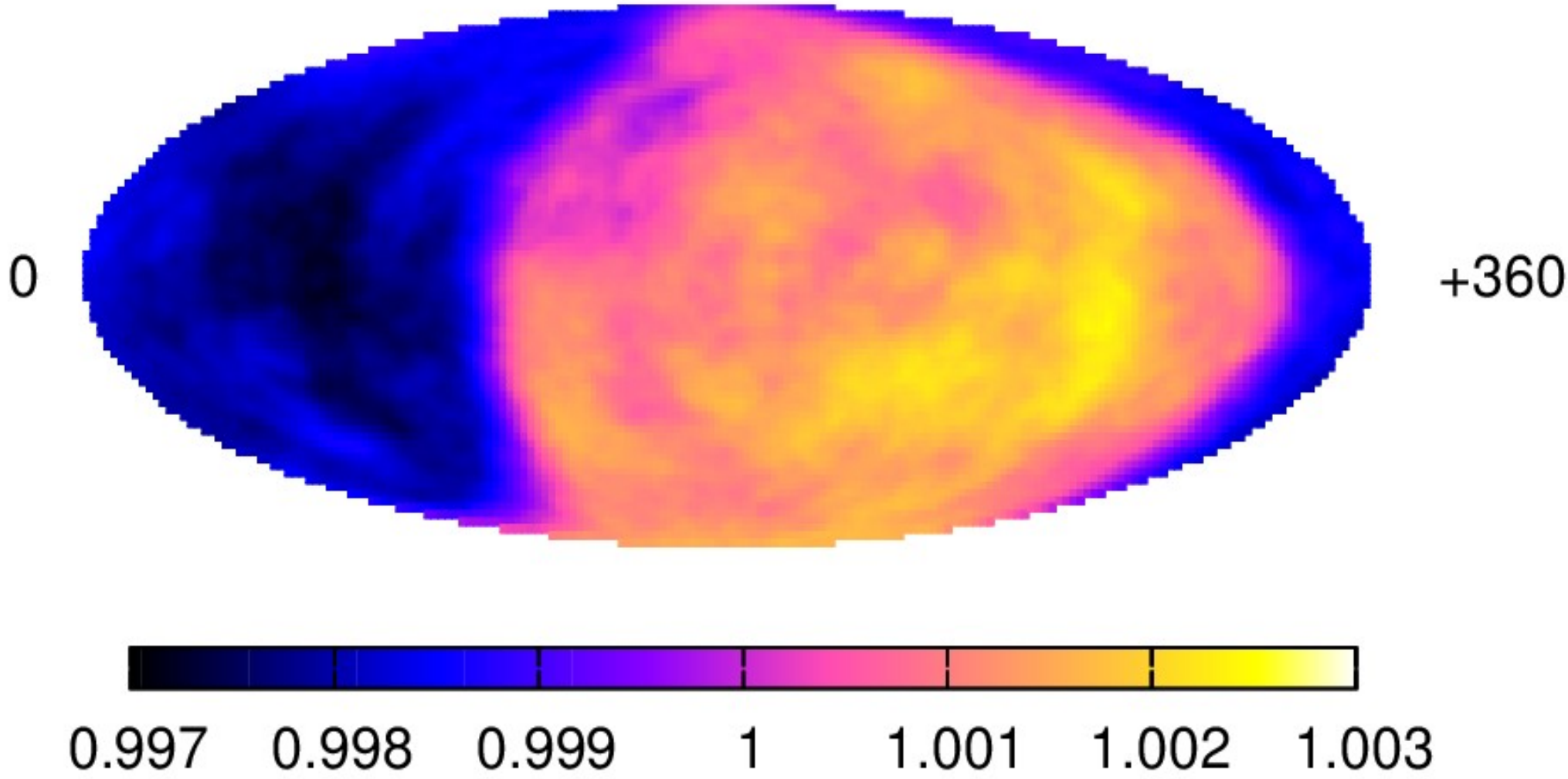

Numerical simulations (Config. 1)

E_{CR} = 10 TeV

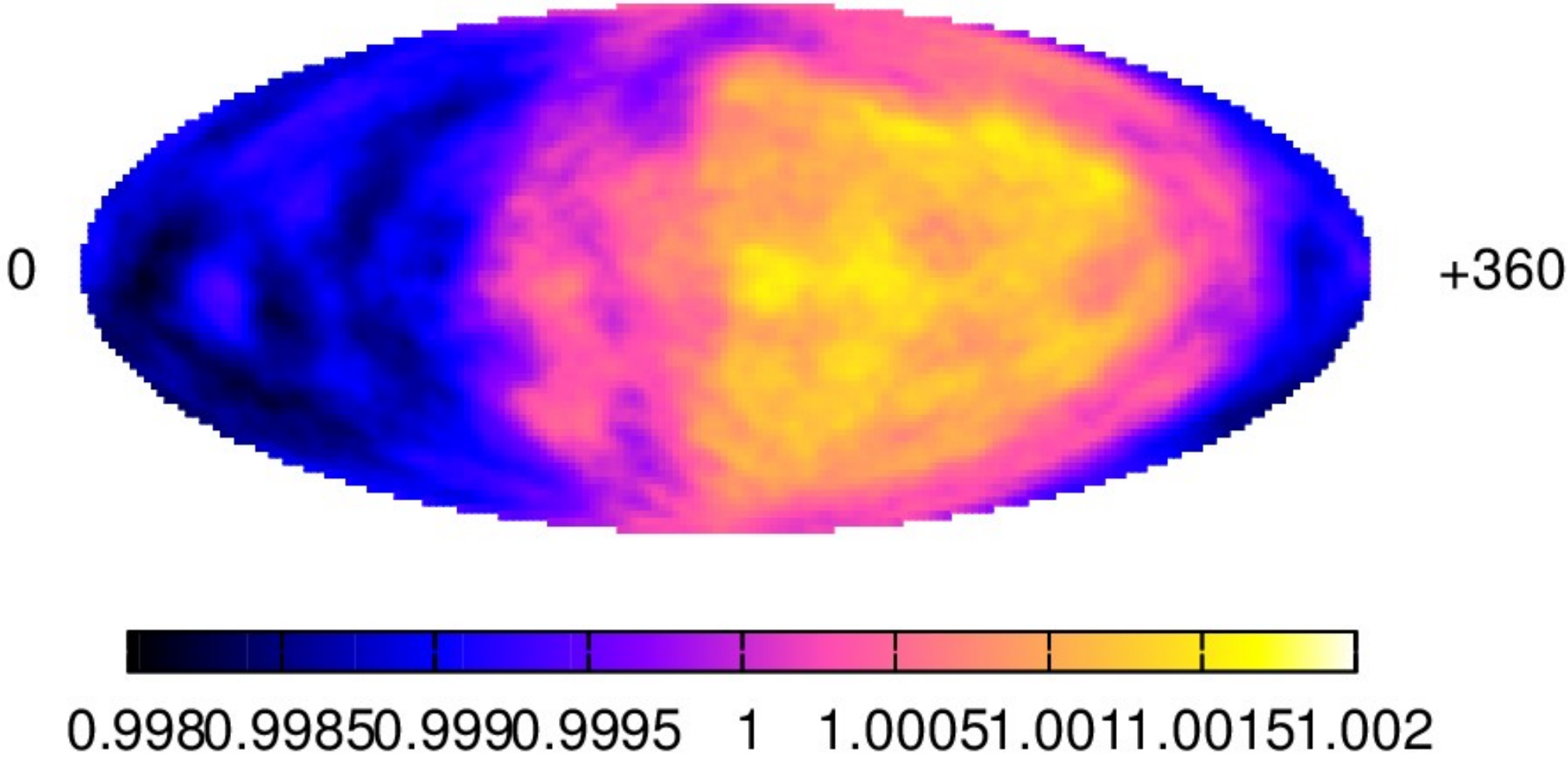

Numerical simulations (Config. 1)

E_{CR} = 3 TeV

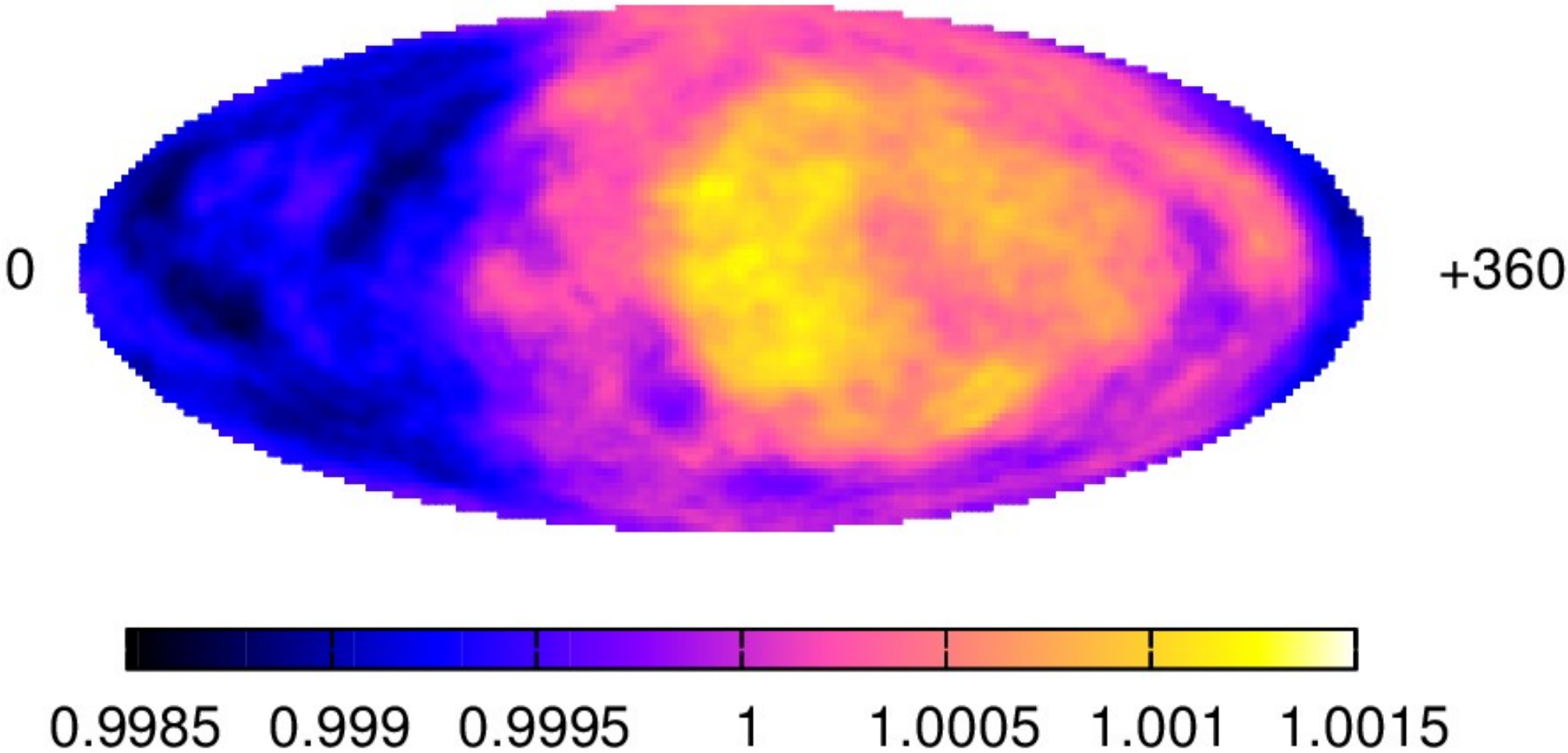

Numerical simulations (Config. 1)

E_{CR} = 3 TeV

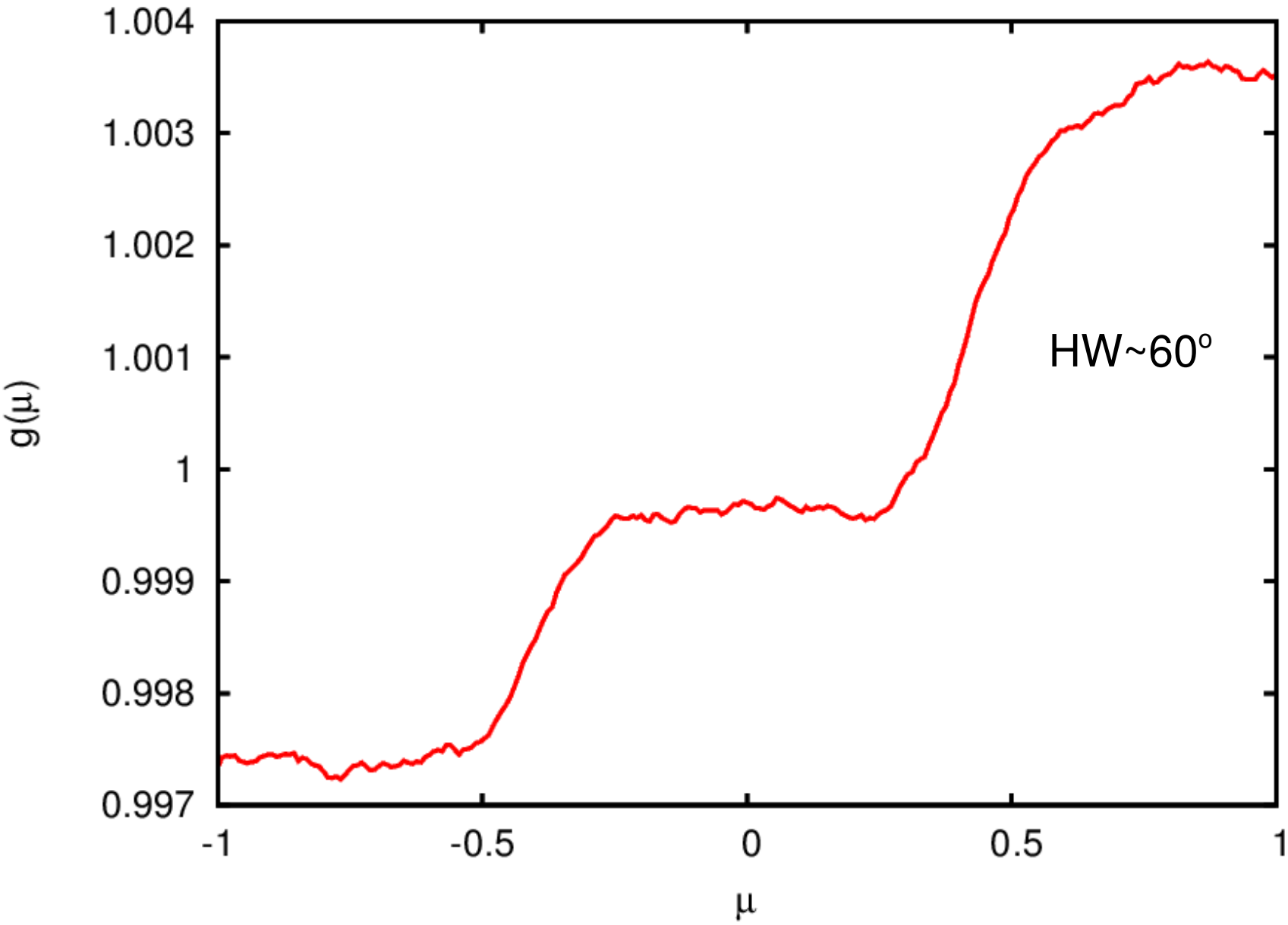

Convergence LSA (Config. 1)

E_{CR} = **3 TeV**

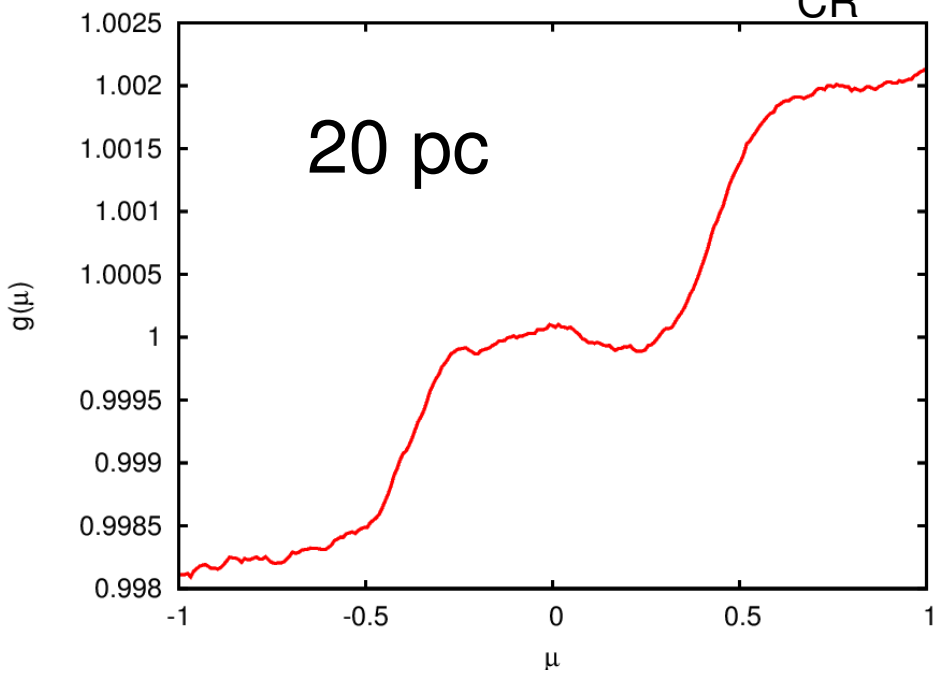

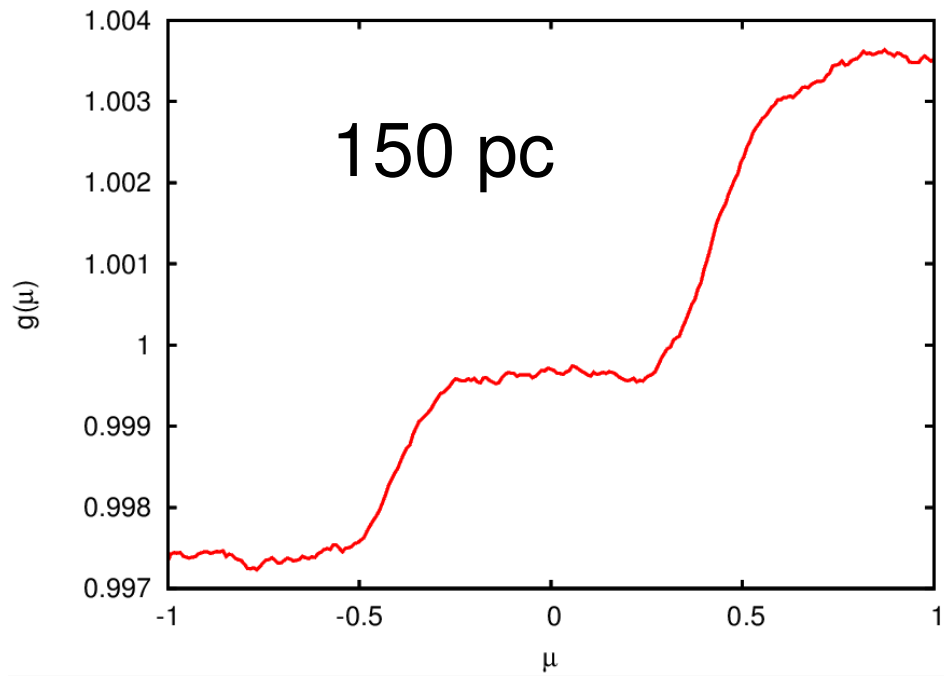

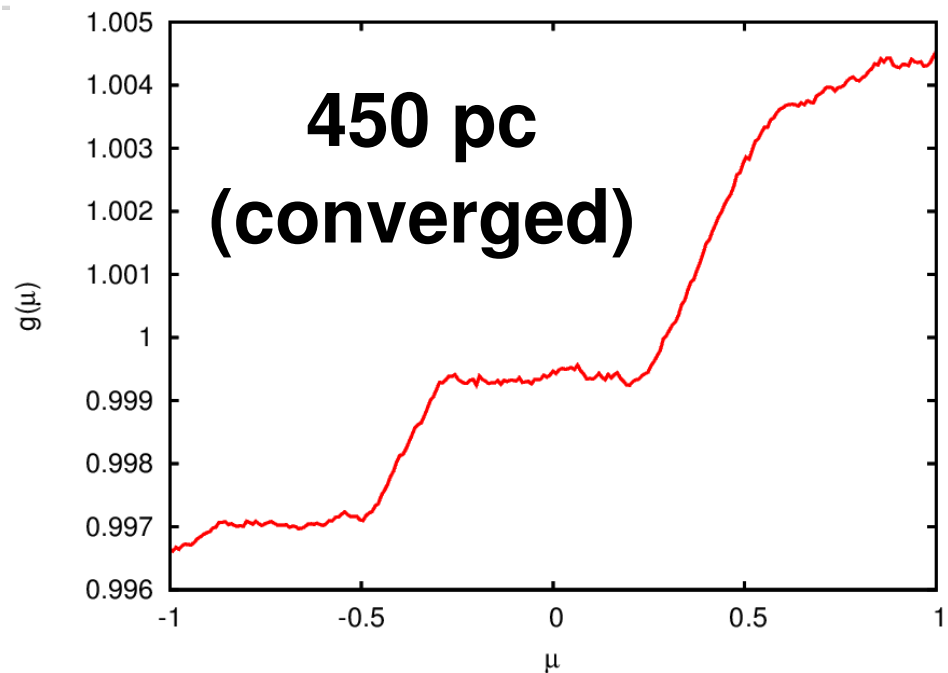

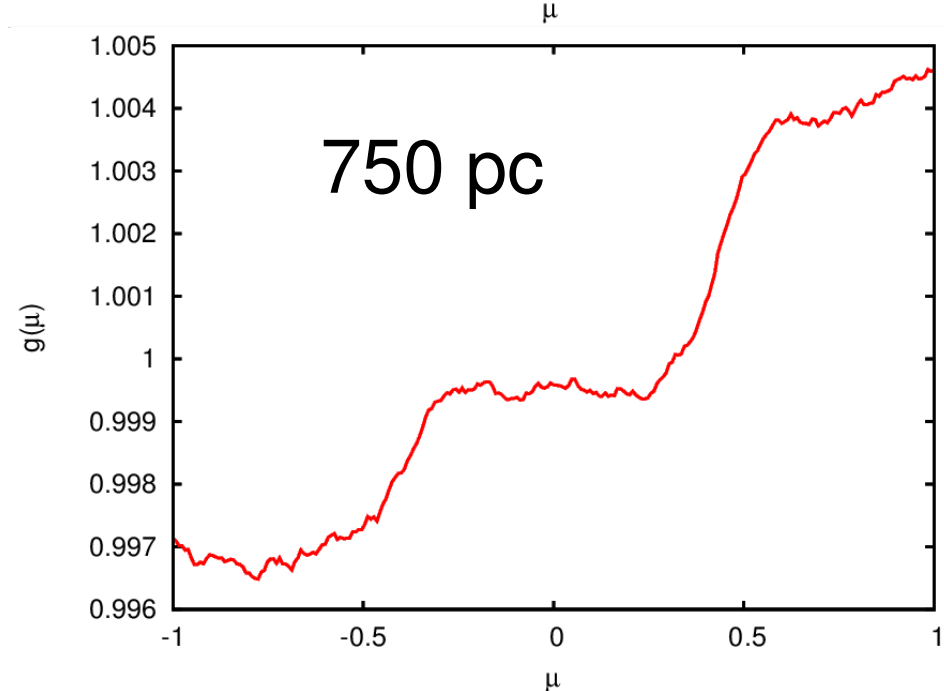

Numerical simulations (Config 2)

E_{CR} = 3 PeV

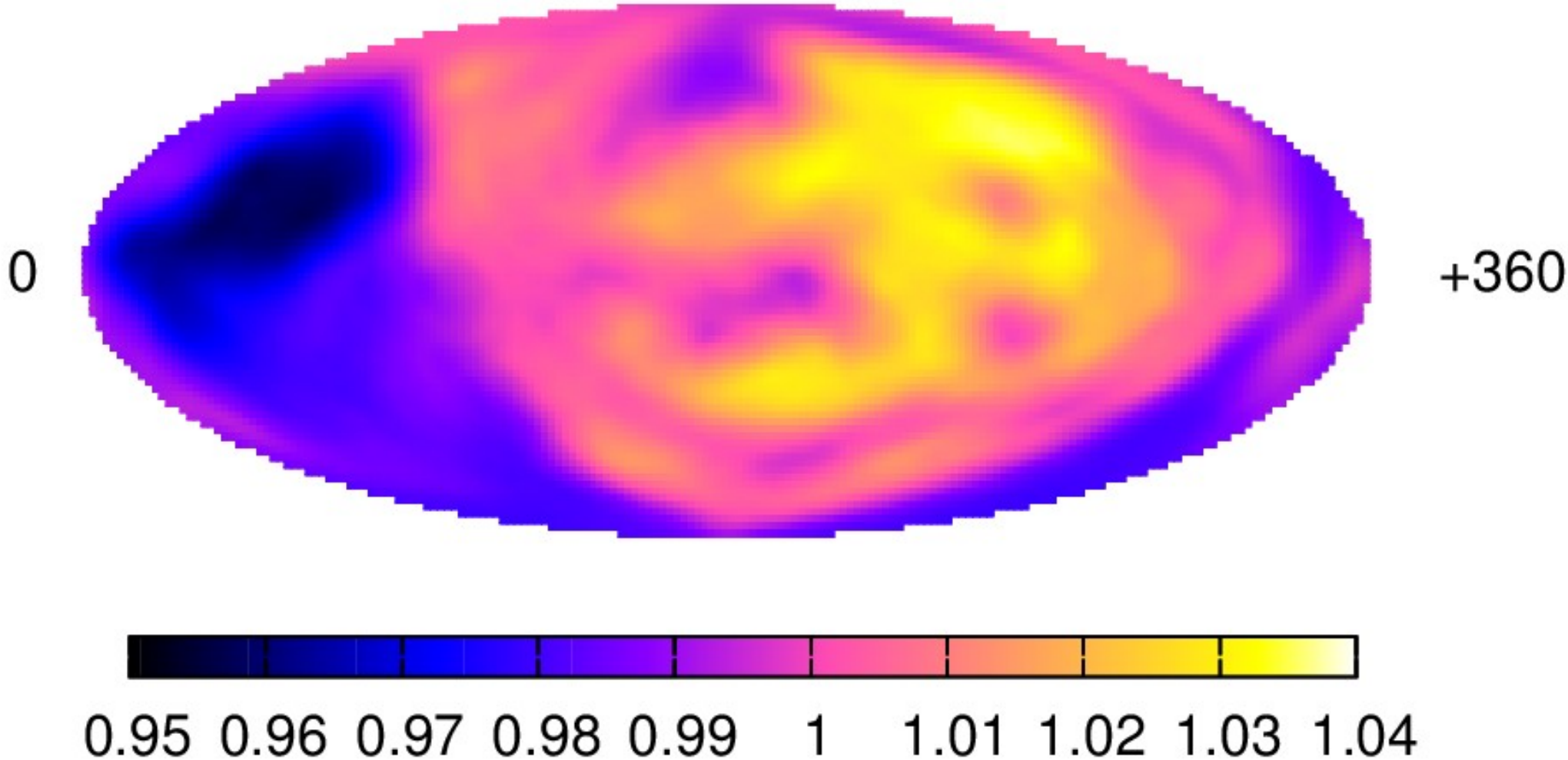

Numerical simulations (Config. 2)

E_{CR} = 1 PeV

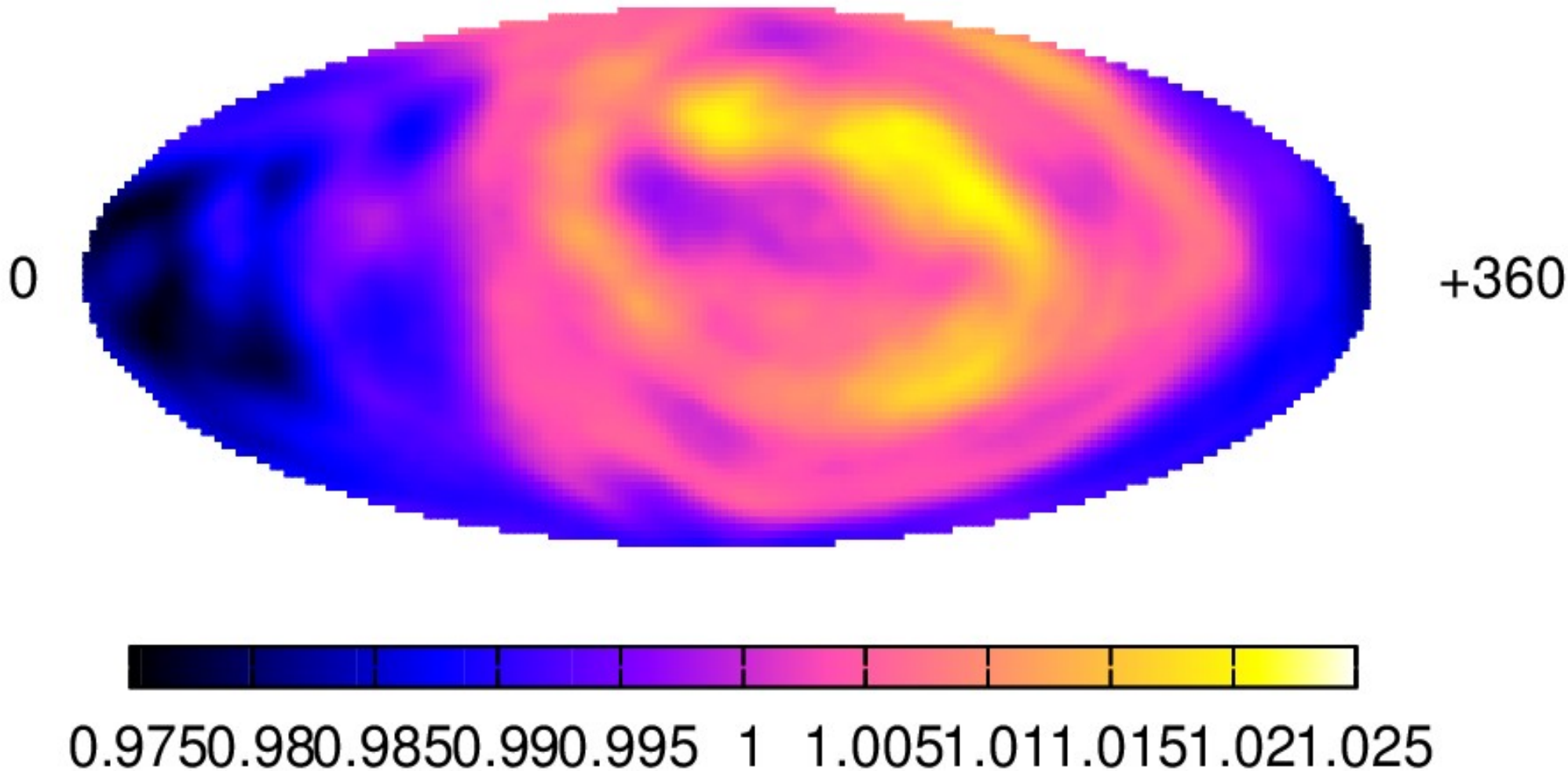

Numerical simulations (Config. 2)

E_{CR} = 300 TeV

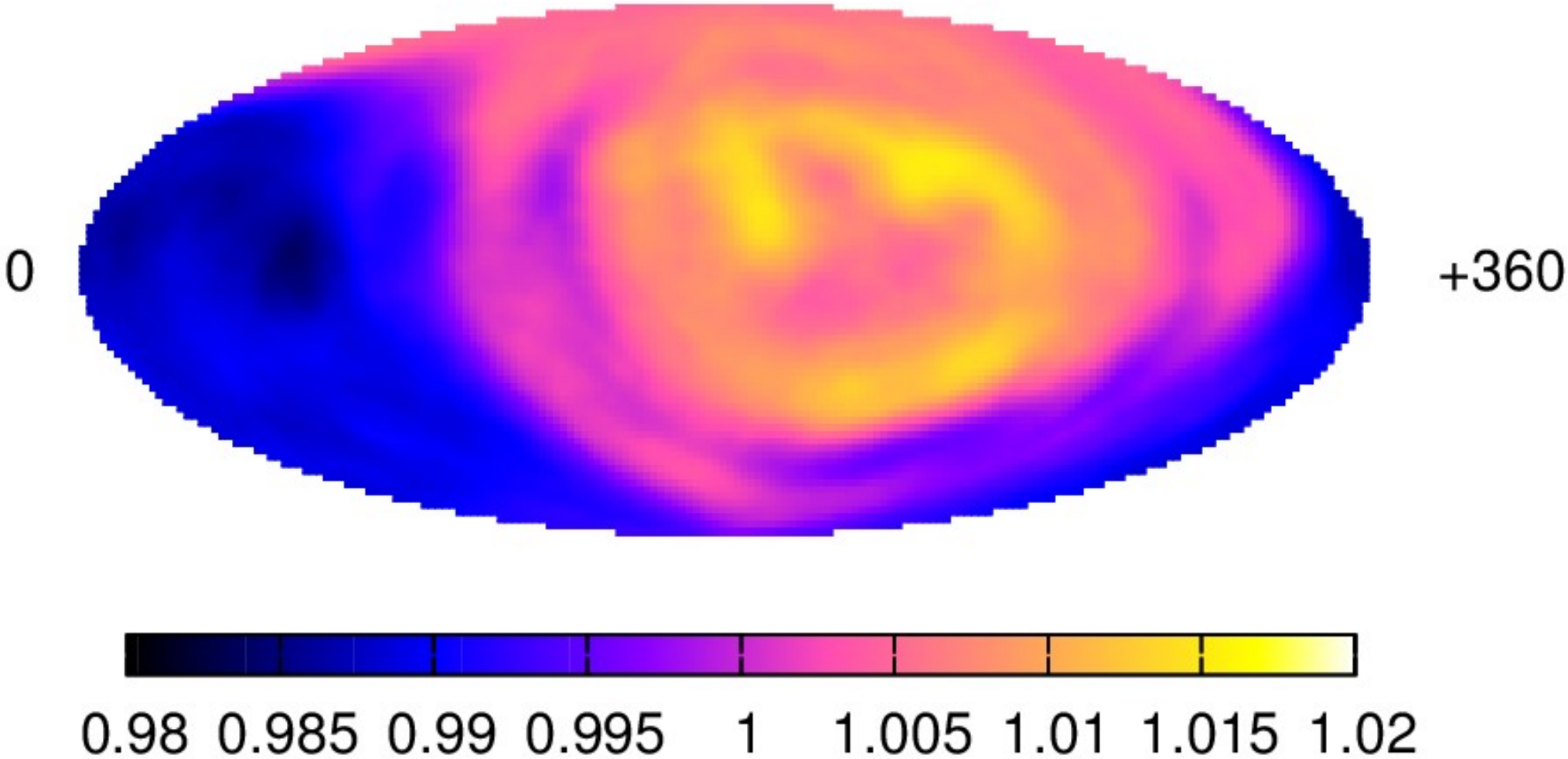

Numerical simulations (Config. 2)

E_{CR} = 100 TeV

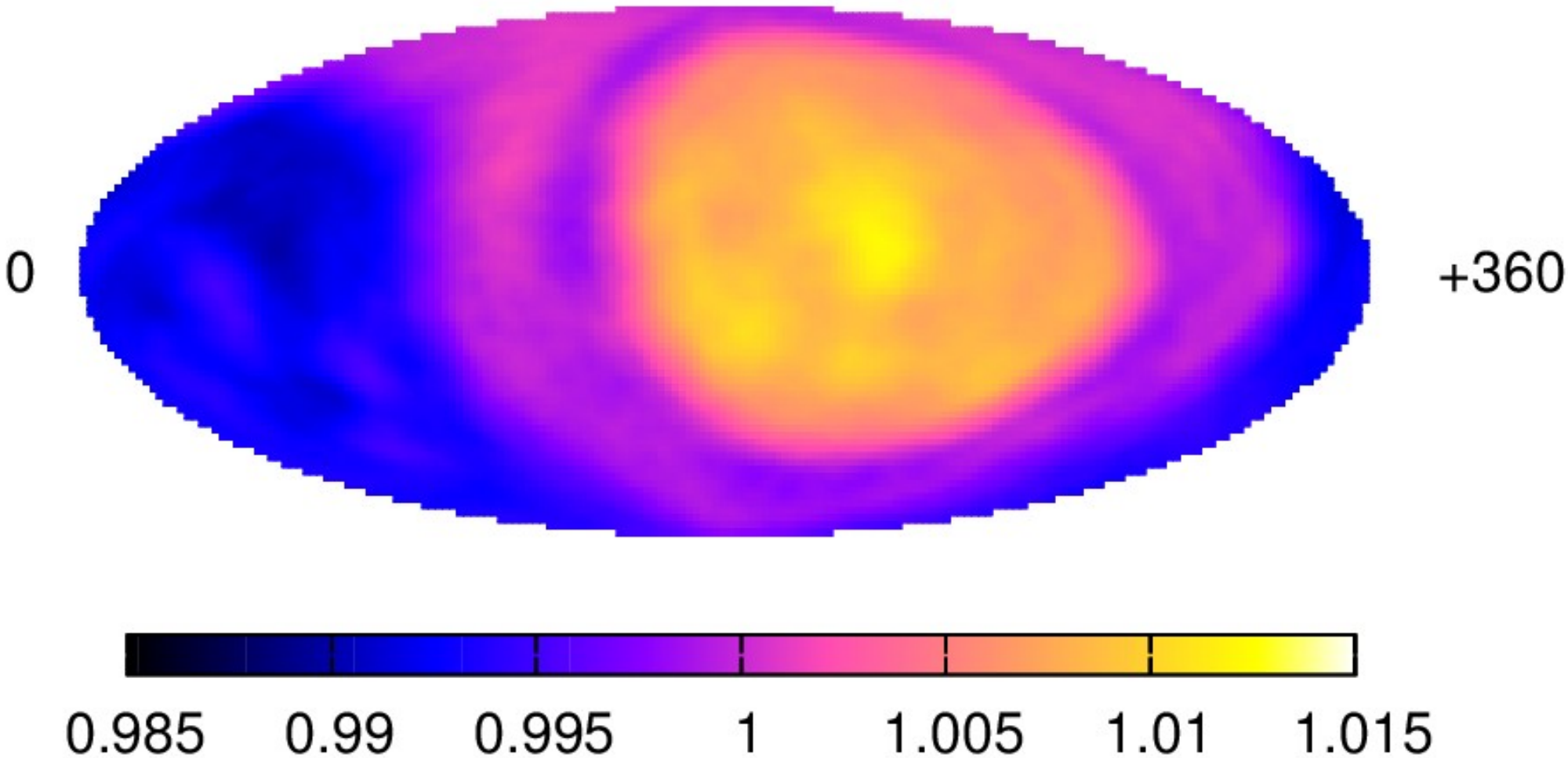

Numerical simulations (Config. 2)

E_{CR} = 30 TeV

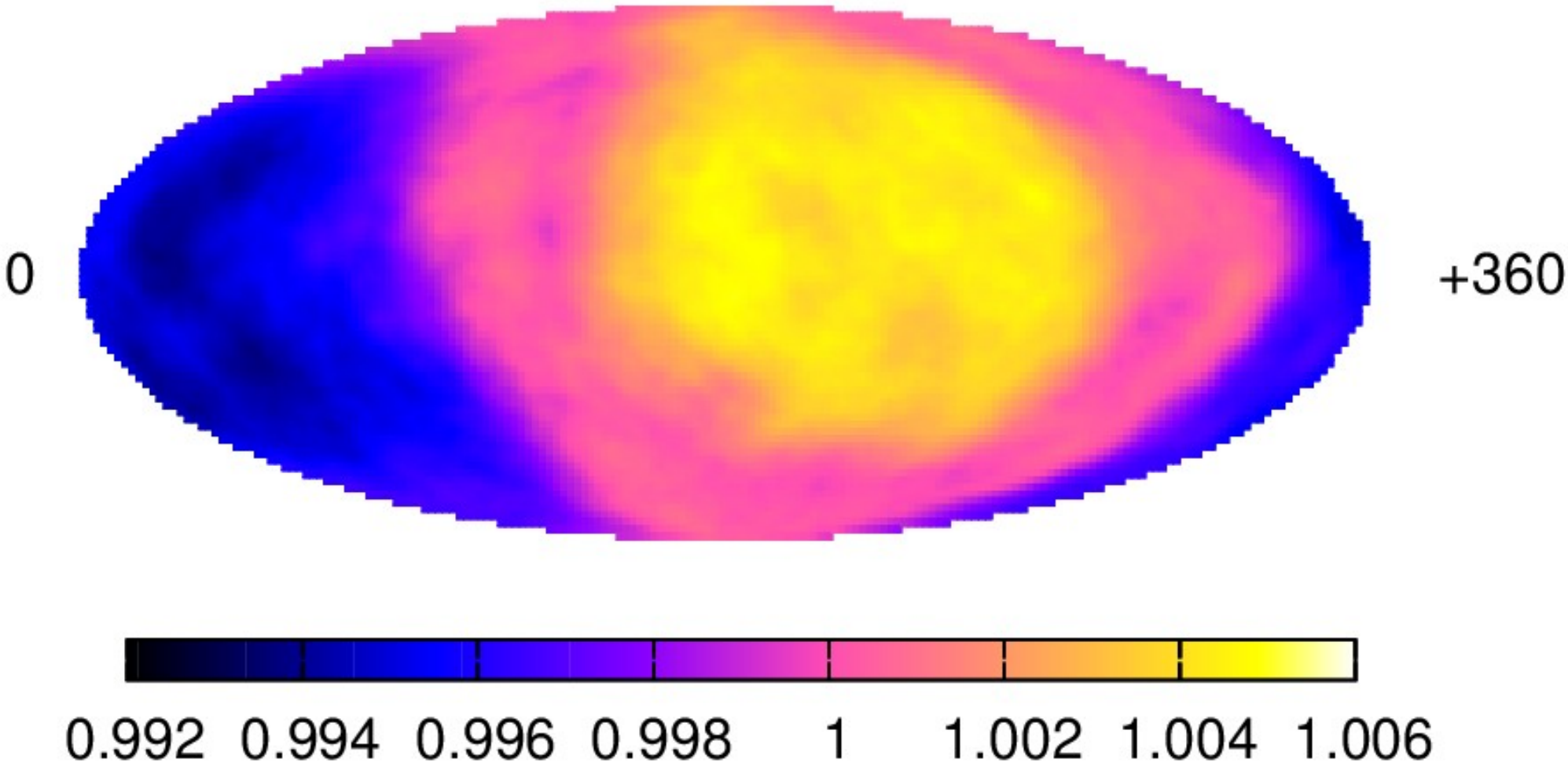

Numerical simulations (Config. 2)

E_{CR} = 10 TeV

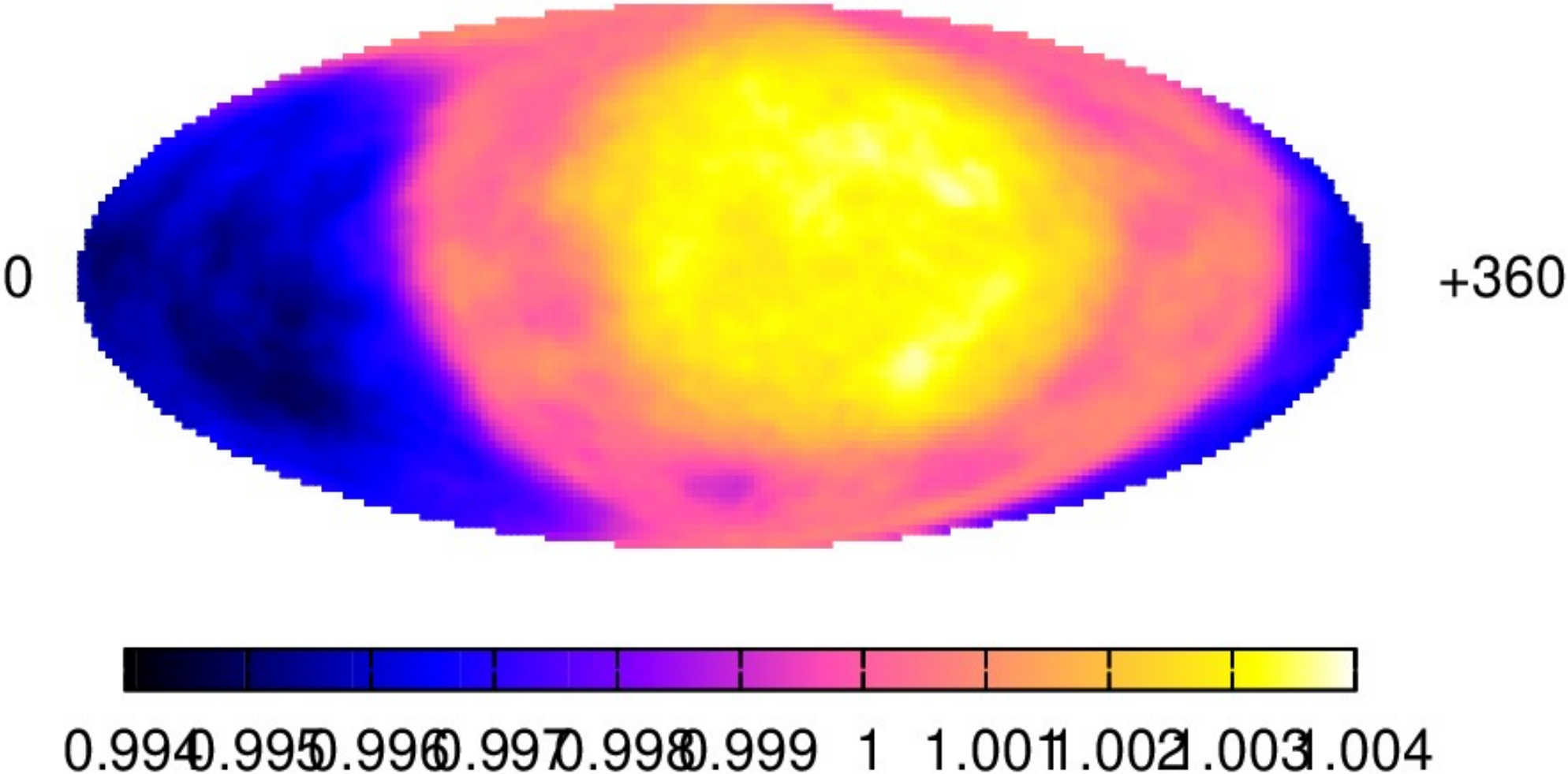

Numerical simulations (Config. 2)

E_{CR} = 3 TeV

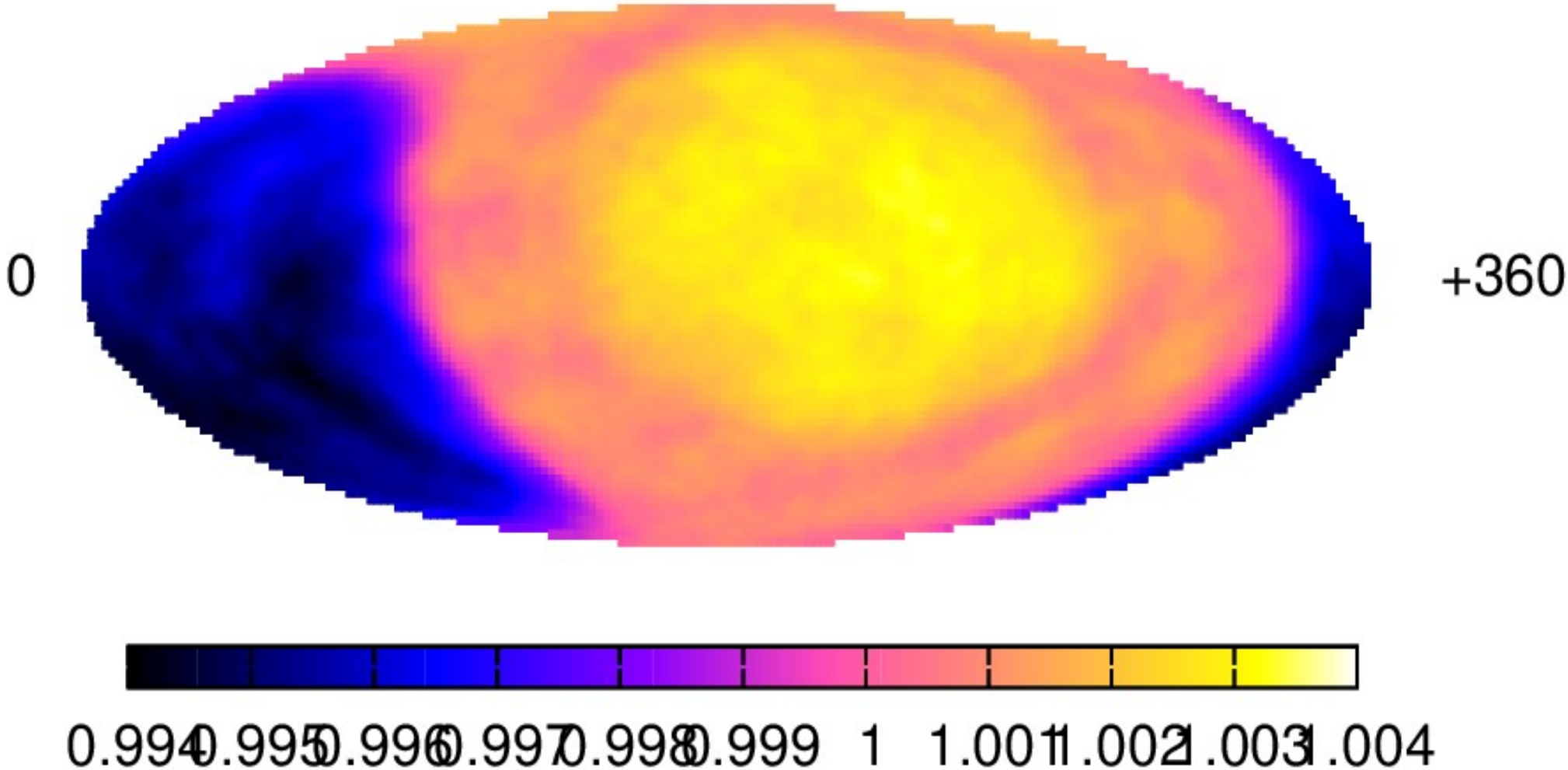

Local magnetic field (Config. 2)

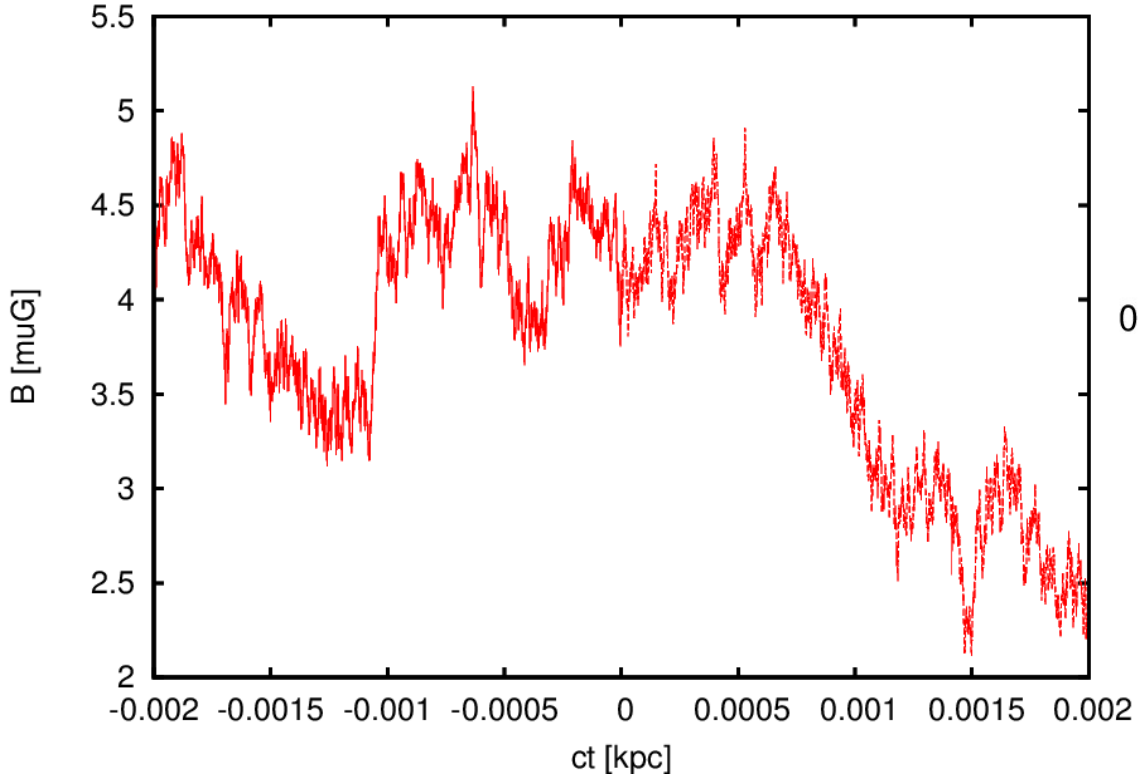

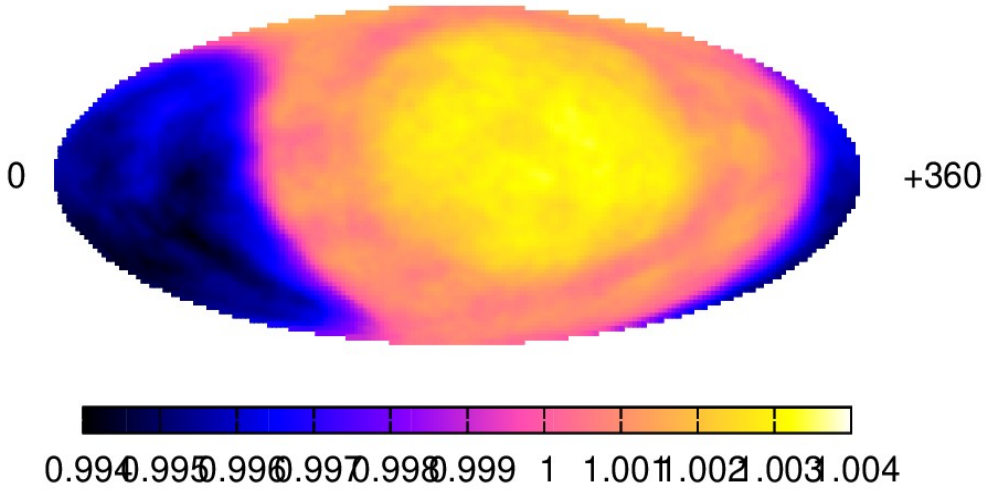

Local magnetic field (Config. 3)

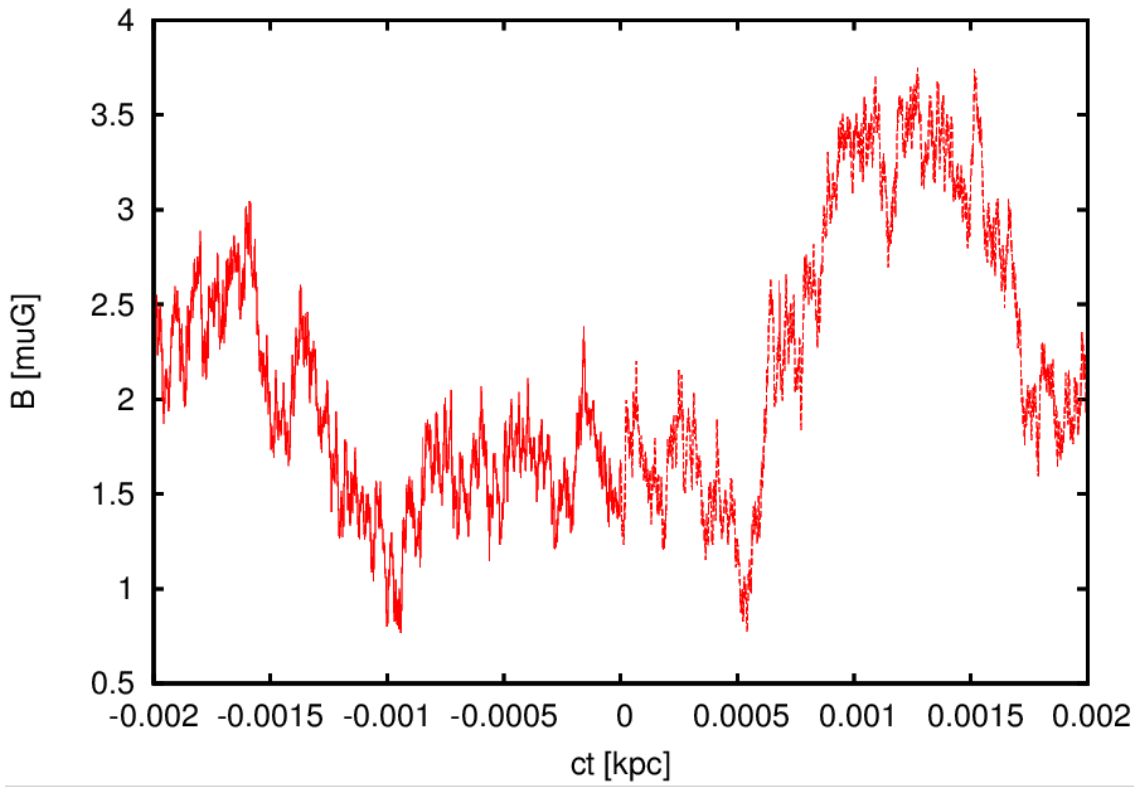

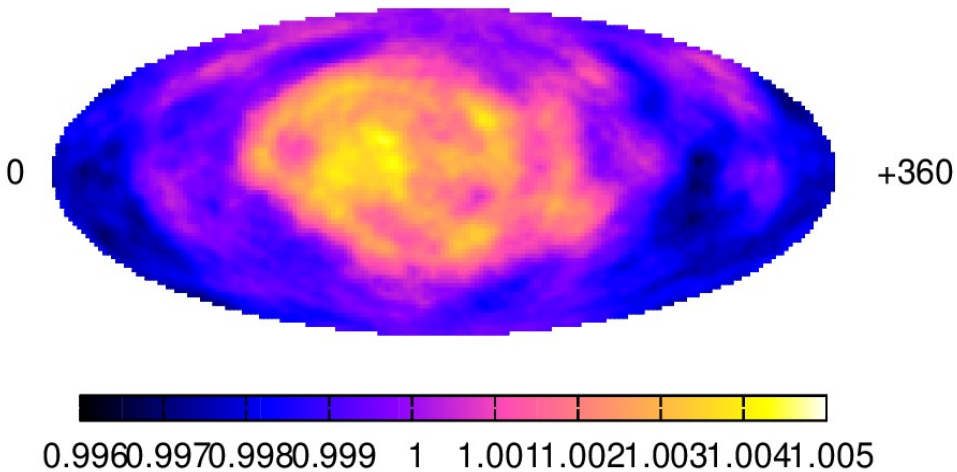

=> Amplitude SSA/LSA is related to *local* δB/B.

Local magnetic field (Config. 4)

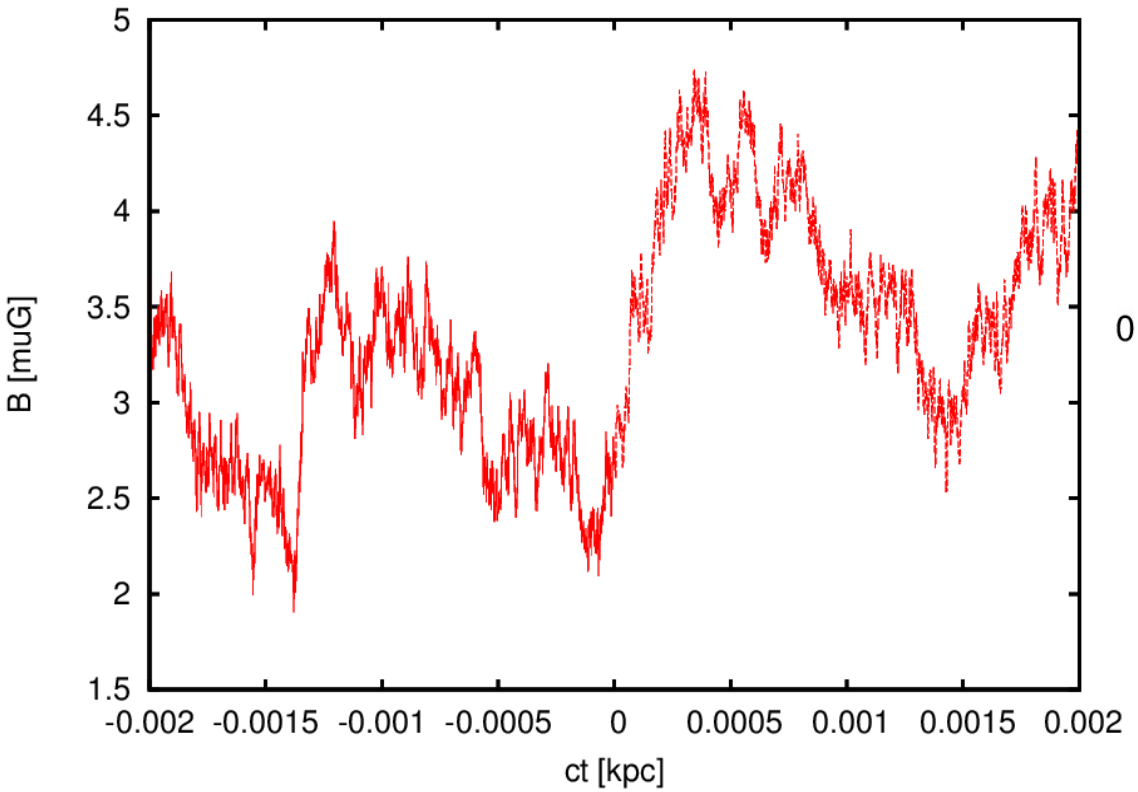

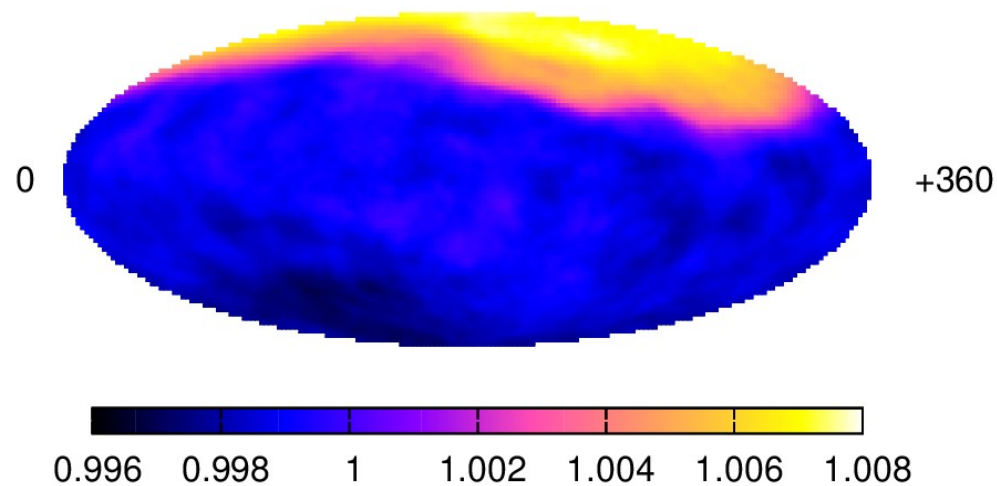

Numerical simulations (Config. 4)

E_{CR} = 3 TeV

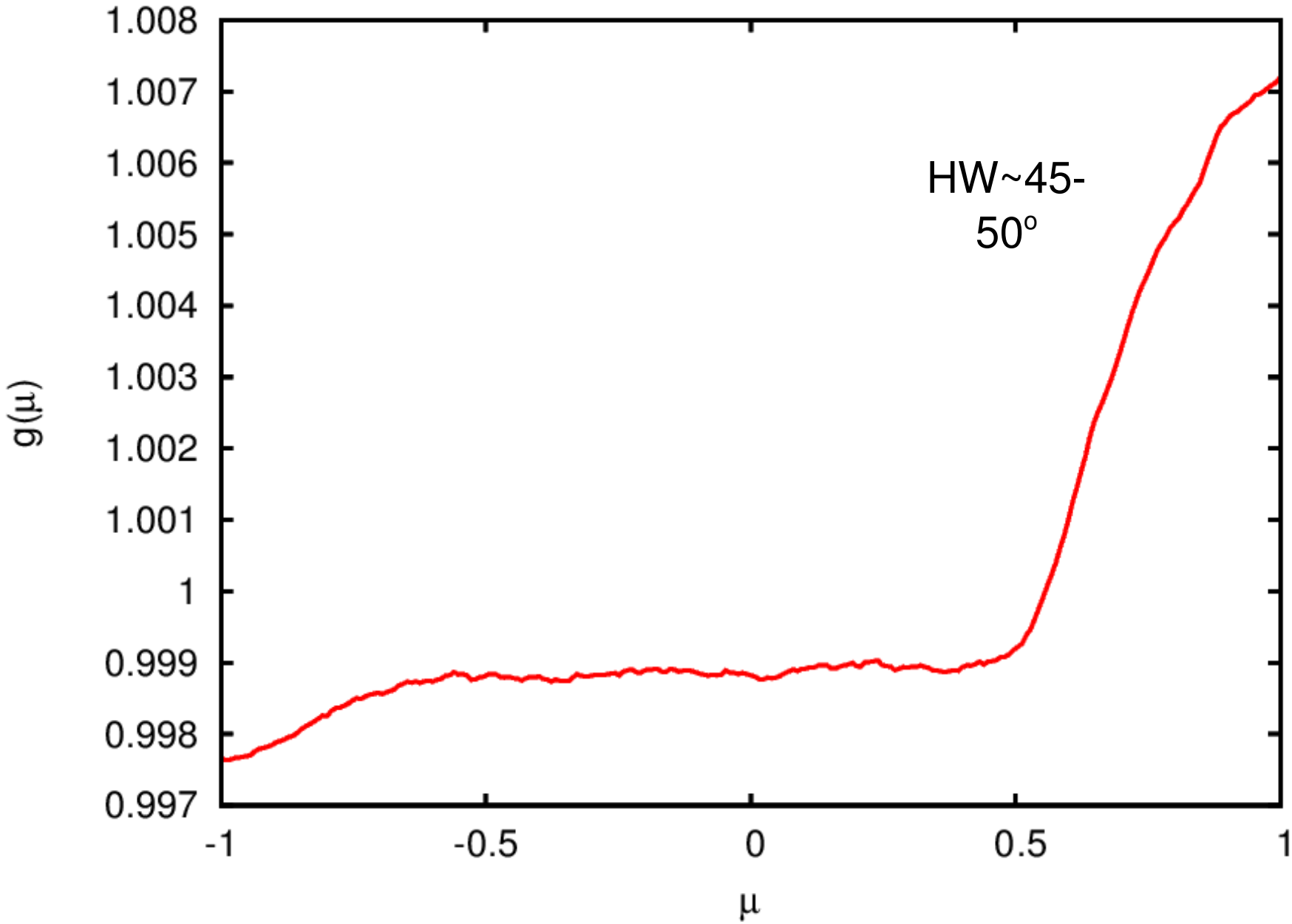

(non-gyrotropic) Small-Scale Anisotropies at 3 TeV

LSA at 3 TeV (Config. 5, 10 pc)

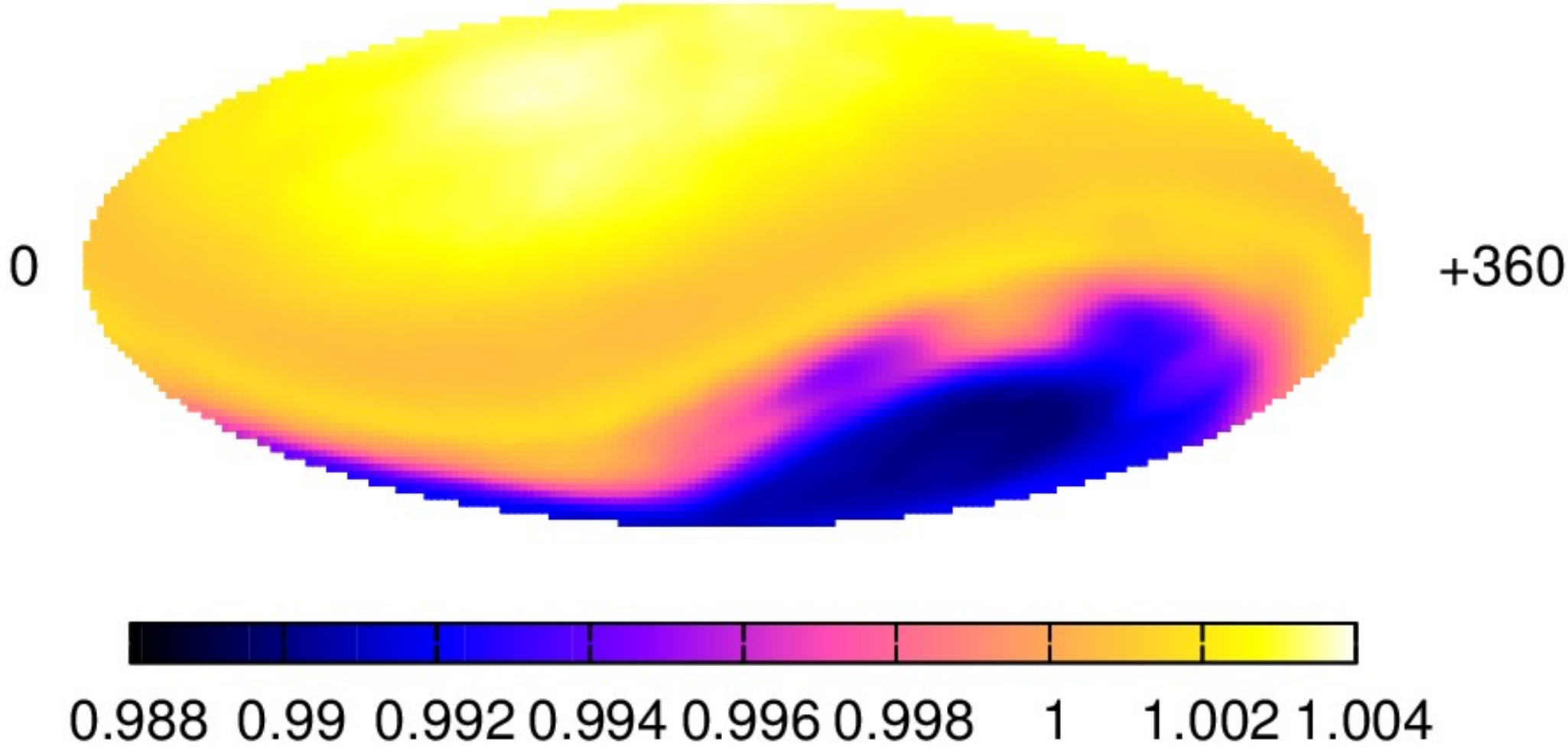

SSA at 3 TeV (Config. 5, 10 pc)

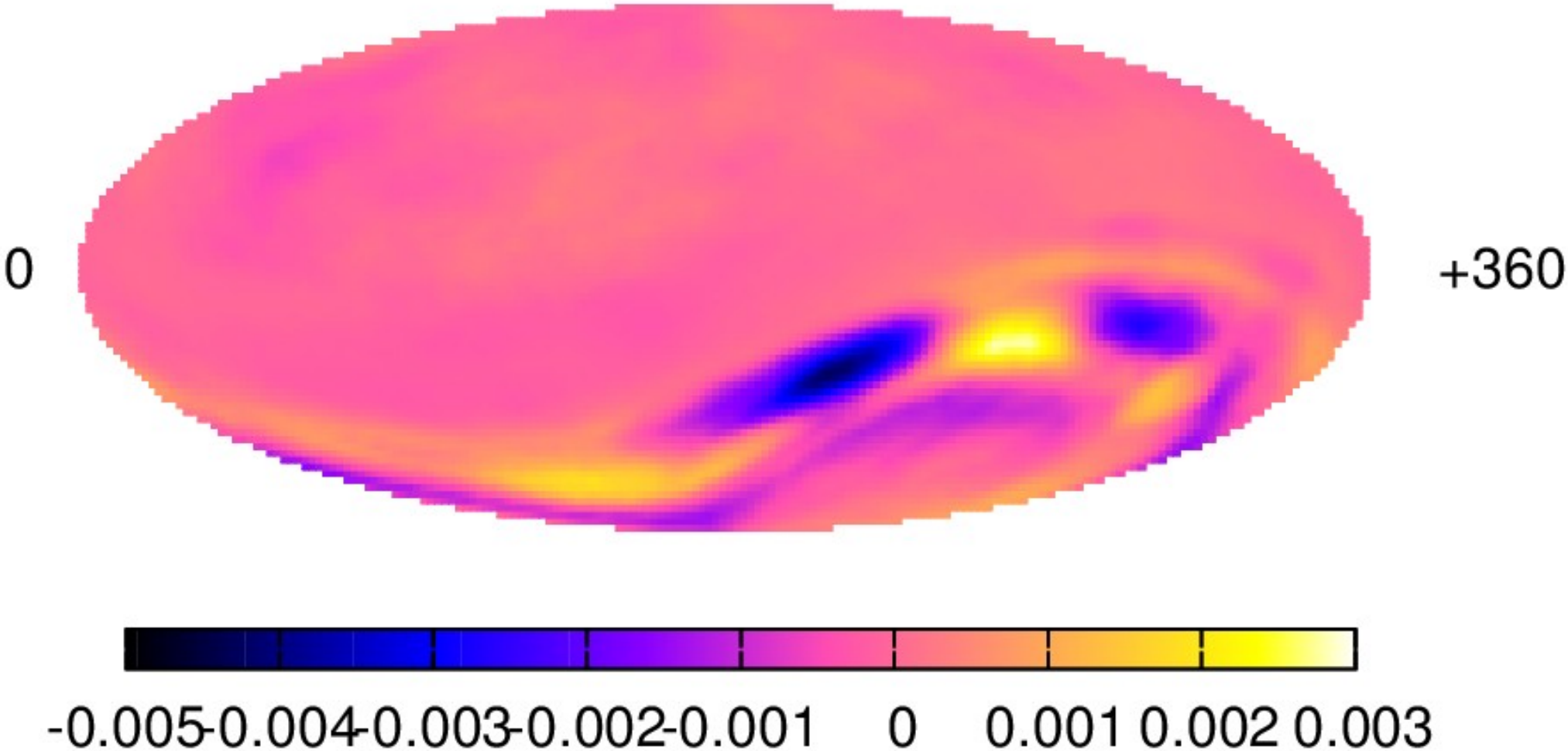

Noise at 3 TeV (Config. 5, 10 pc)

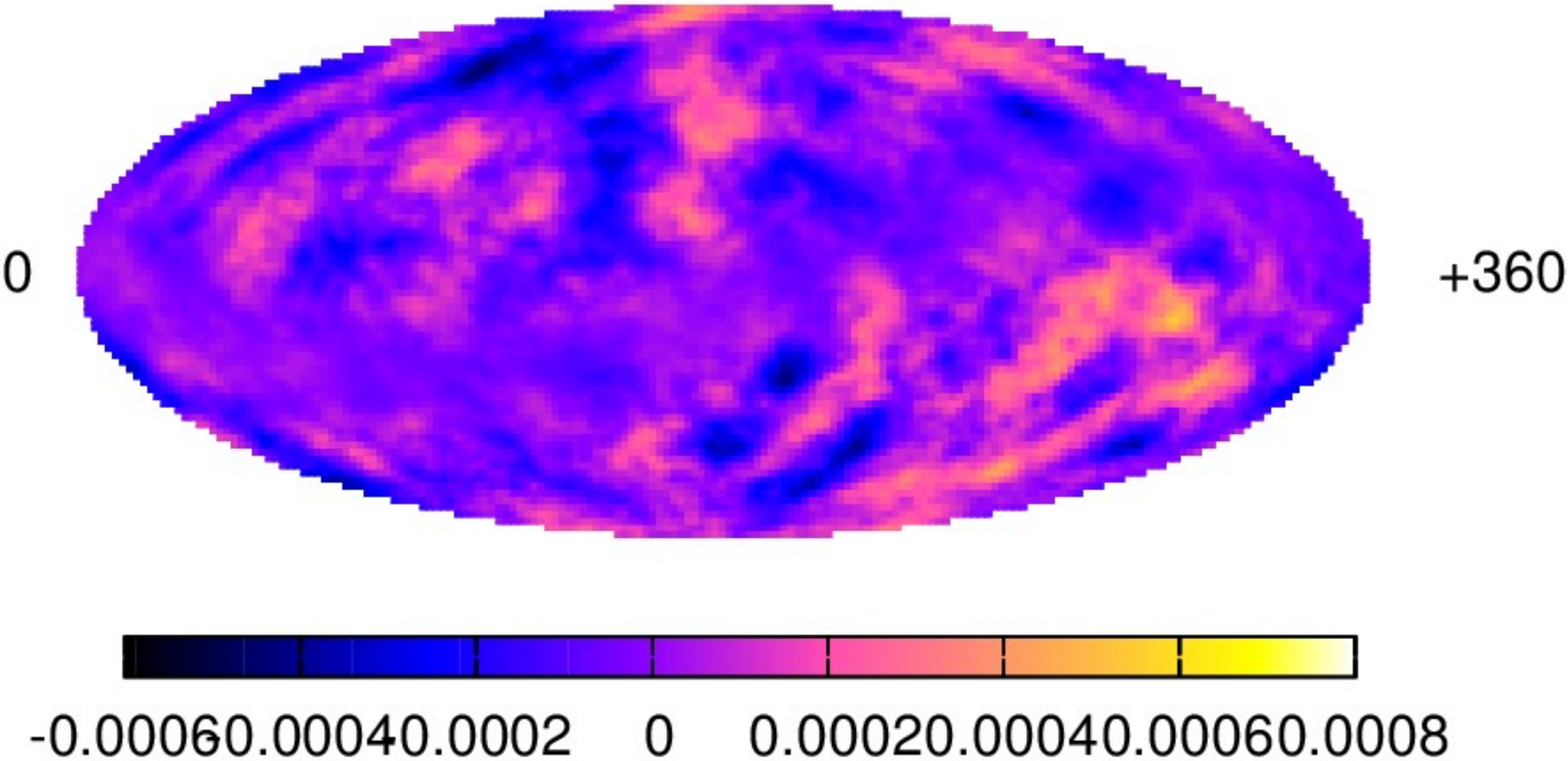

Conclusions (New simulations) :

→ LSA aligns with local B field lines. Gyrotropy assumption ~ OK at E <~ 100 TeV – 1 PeV,

→ Flattening of the LSA in directions perpendicular to field lines. Compatible with moderately broad RFs,

→ LSA shape in μ contains crucial information on the properties of the local turbulence (as expected on theoretical grounds). + and - amplitudes of LSA not nec. symmetric with respect to μ=0,

→ SSA do appear with the correct amplitude at TeV energies. Most prominent SSA appear in regions where $g'(\mu)$ is large. Amplitude also depends on local $\delta B/B$.